

# Infrared multiple photon dissociation spectroscopy of cationized methionine: effects of alkali-metal cation size on gas-phase conformation†

Damon R. Carl,<sup>a</sup> Theresa E. Cooper,<sup>a</sup> Jos Oomens,<sup>b</sup> Jeff D. Steill<sup>b</sup> and P. B. Armentrout<sup>\*a</sup>

Received 14th September 2009, Accepted 2nd December 2009

First published as an Advance Article on the web 19th January 2010

DOI: 10.1039/b919039b

The gas-phase structures of alkali-metal cation complexes of the amino acid methionine (Met) as well as protonated methionine are investigated using infrared multiple photon dissociation (IRMPD) spectroscopy utilizing light generated by a free electron laser. Spectra of  $\text{Li}^+$  (Met) and  $\text{Na}^+$  (Met) are similar and relatively simple, whereas the spectra of  $\text{K}^+$  (Met),  $\text{Rb}^+$  (Met), and  $\text{Cs}^+$  (Met) include distinctive new bands. Measured IRMPD spectra are compared to spectra calculated at the B3LYP/6-311+G(d,p) level of theory to identify the conformations present in the experimental studies. For  $\text{Li}^+$  and  $\text{Na}^+$  complexes, the only conformation present is a charge-solvated, tridentate structure that binds the metal cation to the amine and carbonyl groups of the amino acid backbone and the sulfur atom of the side chain, [N,CO,S]. In addition to the [N,CO,S] conformer, bands corresponding to alkali-metal cation binding to a bidentate zwitterionic structure,  $[\text{CO}_2^-]$ , are clearly present for the  $\text{K}^+$ ,  $\text{Rb}^+$ , and  $\text{Cs}^+$  complexes. Theoretical calculations of the lowest energy conformations of  $\text{Rb}^+$  and  $\text{Cs}^+$  complexes suggest that the experimental spectra could also include contributions from two additional charge-solvated structures, tridentate [COOH,S] and bidentate [COOH]. For  $\text{H}^+$  (Met), the IRMPD action spectrum is reproduced by multiple low-energy [N,CO,S] conformers, in which the protonated amine group hydrogen bonds to the carbonyl oxygen atom and the sulfur atom of the amino acid side chain. These [N,CO,S] conformers only differ in their side-chain orientations.

## Introduction

Fundamental interactions between biologically relevant metal ions and small molecules can have a profound effect on the function of complex biological processes. For example, the interactions between potassium ions and sulfur-containing amino acid methionine (Met) in the outer pore region of inward rectifying  $\text{K}^+$  (Kir) ion channels are an important controlling factor in the selective passage of monocations.<sup>1</sup>

<sup>a</sup> Department of Chemistry, University of Utah, Salt Lake City, UT 84112, USA. E-mail: armentrout@chem.utah.edu

<sup>b</sup> FOM Institute for Plasma Physics "Rijnhuizen", Edisonbaan 14, 3439 MN Nieuwegein, The Netherlands

† Electronic supplementary information (ESI) available: A description of the structures of Met and  $\text{M}^+$  (Met) for  $\text{M}^+ = \text{Li}^+, \text{Na}^+, \text{K}^+, \text{Rb}^+, \text{and } \text{Cs}^+$ . One figure (S1) depicting the Gibbs free energy at 298 K calculated at the B3LYP/6-311+G(2d,2p)//B3LYP/6-311+G(d,p) ( $\text{M}^+ = \text{Li}^+, \text{Na}^+, \text{K}^+$ ) and B3LYP/HW\*/6-311+G(2d,2p)//B3LYP/HW\*/6-311+G(d,p) ( $\text{M}^+ = \text{Rb}^+ \text{ and } \text{Cs}^+$ ) levels of theory. One table (S1) providing 0 K relative energies calculated at the R/HW\*/6-311+G(2d,2p) and R/Def2TZVP levels of theory, where R = B3LYP, B3P86, and MP2(full), for eight conformations of  $\text{Rb}^+$  (Met) and  $\text{Cs}^+$  (Met). Two tables (S2 and S3) providing geometric parameters (bond lengths, bond angles, and dihedral angles) for low-energy structures of  $\text{M}^+$  (Met). Ten tables (S4–S13) providing the vibrational frequencies and IR intensities for various conformations of  $\text{M}^+$  (Met) calculated at the B3LYP/6-311+G(d,p) ( $\text{M}^+ = \text{Li}^+, \text{Na}^+, \text{K}^+$ ) and B3LYP/HW\*/6-311+G(d,p) ( $\text{M}^+ = \text{Rb}^+ \text{ and } \text{Cs}^+$ ) levels of theory. Two tables (S14 and S15) providing the vibrational frequencies and IR intensities for four [N,CO,S] and four [N,OH,S] conformers of  $\text{H}^+$  (Met) calculated at the B3LYP/6-311+G(d,p) level.

Recently, the pairwise interactions between Met with the alkali-metal cations,  $\text{Li}^+$ ,  $\text{Na}^+$ , and  $\text{K}^+$ , have been investigated using guided ion beam mass spectrometry.<sup>2</sup> Quantitative bond dissociation energies were determined and found to be consistent with theoretical values predicted for the ground state conformations, charge-solvated structures involving tridentate bonding of the metal ion to the amine and carbonyl groups of the amino acid backbone and the side-chain sulfur atom, [N,CO,S] (see nomenclature below), for  $\text{Li}^+$  and  $\text{Na}^+$ . For  $\text{Li}^+$  (Met) and  $\text{Na}^+$  (Met), the [N,CO,S] ground state lies well below ( $> 10 \text{ kJ mol}^{-1}$ ) any other conformations such that quantitative measurements are sufficient to determine the identity of the complexes formed experimentally.<sup>2</sup> Calculations indicate that the energy differences between the ground state and higher energy conformations decrease as the metal cations become heavier. For example, MP2(full) calculations predict a ground state of [N,CO,S] for  $\text{K}^+$  complexed to Met, but density functional theory calculations indicate the ground state is bidentate with  $\text{K}^+$  bound to the carboxylate moiety of the zwitterionic  $[\text{CO}_2^-]$  conformation and the  $\text{NH}_3^+$  group hydrogen bonds to the side-chain sulfur atom.<sup>2</sup> At both levels of theory, the [N,CO,S] and  $[\text{CO}_2^-]$  conformers are separated by less than  $3 \text{ kJ mol}^{-1}$ . Low-energy conformations are likely present for  $\text{Rb}^+$  and  $\text{Cs}^+$  complexed to Met as well. As such, threshold collision-induced dissociation measurements are unable to distinguish between small differences in conformational energy.

Infrared multiple photon dissociation (IRMPD) action spectroscopy can be used to examine the presence of specific conformations as a function of metal cation size. Previous IRMPD studies on  $M^+(\text{Ser})^3$  and  $M^+(\text{Thr})^4$  have found that the  $M^+ = \text{Li}^+$  and  $\text{Na}^+$  complexes are bound in a tridentate  $[\text{N},\text{CO},\text{OH}]$  conformer, whereas spectra for  $M^+ = \text{K}^+$  and  $\text{Rb}^+$  include evidence of bidentate  $[\text{COOH}]$  conformations. Additionally, the spectra for  $\text{Cs}^+$  serine and threonine complexes also include contributions from a zwitterionic  $[\text{CO}_2^-]$  conformer. For  $M^+(\text{Arg})$ , the transition from ground state charge-solvated to zwitterionic conformation occurs at  $\text{Na}^+(\text{Arg})$ .<sup>5</sup> The IRMPD action spectra of  $M^+(\text{Asn})$  maintain the charge-solvated tridentate  $[\text{N},\text{CO},\text{CO}]$  conformation throughout the alkali cation series, but also include spectral contributions from the  $[\text{COOH},\text{CO}]$  conformer for  $\text{K}^+(\text{Asn})$  to  $\text{Cs}^+(\text{Asn})$ .<sup>6</sup> A similar progression is seen in IRMPD studies of  $M^+(\text{Gln})$ ,<sup>7</sup>  $M^+(\text{Trp})$ <sup>8</sup> and  $M^+(\text{Lys})$ <sup>9</sup> transition from tridentate to bidentate conformers as the metal ion becomes heavier, but still maintain charge-solvated complexes. In the present study, we examine whether such trends are influenced by having a side chain with a sulfur-containing functional group, which tends to bind metal cations at different angles compared to analogous ether functional groups.<sup>2</sup> Thus, we measure the IRMPD action spectra for dissociation of  $M^+(\text{Met})$  complexes, where  $M^+ = \text{Li}^+, \text{Na}^+, \text{K}^+, \text{Rb}^+, \text{Cs}^+$ , and  $\text{H}^+$ . The conformations are identified by comparing the experimental action spectra to IR spectra predicted by quantum chemical calculations of the low-lying structures of the  $M^+(\text{Met})$  complexes optimized at the B3LYP/6-311+G(d,p) level of theory.

## Experimental and computational section

### Mass spectrometry and photodissociation

A 4.7 T Fourier transform ion cyclotron resonance (FTICR) mass spectrometer was used in these experiments and has been described in detail elsewhere.<sup>10–12</sup> Tunable radiation for the photodissociation experiments is generated by the free electron laser for infrared experiments (FELIX).<sup>13</sup> For the present experiments, spectra were recorded over the wavelength range 19.4  $\mu\text{m}$  (520  $\text{cm}^{-1}$ ) to 5.5  $\mu\text{m}$  (1820  $\text{cm}^{-1}$ ). Pulse energies were around 50 mJ per macropulse of 5  $\mu\text{s}$  duration, although they fell off to about 20 mJ toward the blue edge of the scan range. Complexes were irradiated for 2.5 seconds, which corresponds to interaction with approximately 12 macropulses. The fwhm bandwidth of the laser was typically 0.5% of the central wavelength. Methionine was obtained from Aldrich. Cationized amino acids were formed by electrospray ionization using a Micromass Z-Spray source and a solution of 1 mM Met and 1 mM alkali-metal chloride (or 1 mM acetic acid for  $\text{H}^+(\text{Met})$ ) in 70% : 30% MeOH :  $\text{H}_2\text{O}$ . Solution flow rates were about 10  $\mu\text{L min}^{-1}$  and the electrospray needle was held at a voltage of 3250 V. Ions were accumulated in a hexapole trap for about 4 s prior to being injected into the ICR cell *via* an rf octopole ion guide. Electrostatic switching of the dc bias of the octopole, where a dc bias voltage is superimposed on the full length of all octopole rods, results in there being no change in the dc electric field along the axis of the ion guide.<sup>12</sup> This decelerates

the ions exiting the octopole such that they can be captured in the ICR cell without a gas pulse and collisional heating of the ions is avoided.<sup>12</sup>

### Computational details

In previous work,<sup>2</sup> Armentrout *et al.* examined likely conformers for  $\text{Li}^+(\text{Met})$ ,  $\text{Na}^+(\text{Met})$ , and  $\text{K}^+(\text{Met})$  using a simulated annealing procedure that combines annealing cycles with quantum chemical calculations.<sup>14</sup> The same procedure is used here for  $\text{H}^+(\text{Met})$  complexes. Briefly, the AMBER program and the AMBER force field based on molecular mechanics<sup>15</sup> were used to search for possible stable structures in each system's conformational space. All possible structures identified this way were subsequently optimized using NWChem<sup>16</sup> at the HF/3-21G level.<sup>17,18</sup> Unique structures for each system within 50  $\text{kJ mol}^{-1}$  of the lowest energy structure ( $\sim 50$  for each complex) were optimized using Gaussian 03<sup>19</sup> at the B3LYP/6-31G(d) level of theory<sup>20,21</sup> with the "loose" keyword (maximum step size 0.01 au and an RMS force of 0.0017 au) to facilitate convergence. Unique structures obtained from this procedure were then chosen for higher-level geometry optimization and frequency calculations using density functional theory (DFT) at the B3LYP/6-311G(d,p) level of theory.<sup>22,23</sup> This level of theory has been shown to provide a reasonable structural description of comparable metal–ligand systems.<sup>3,4,6</sup> Here, we have altered the results slightly by reoptimizing at the B3LYP/6-311+G(d,p) level of theory. Only small changes are observed as bond lengths typically change by  $< 0.03$  Å, bond angles by  $< 1^\circ$ , and relative energies of different conformers are within about 3  $\text{kJ mol}^{-1}$ . Single point energy calculations were carried out for the 6–10 most stable structures at the B3LYP, B3P86, and MP2(full) levels using the 6-311+G(2d,2p) basis set.<sup>22</sup> Zero-point vibrational energy (ZPE) corrections were determined using vibrational frequencies calculated at the B3LYP/6-311+G(d,p) level scaled by a factor of 0.9804.<sup>24</sup>

For the  $\text{Rb}^+(\text{Met})$  and  $\text{Cs}^+(\text{Met})$  complexes studied here, all conformations considered previously for  $\text{K}^+(\text{Met})$  were used as starting points for geometry and vibrational frequency calculations optimized at the B3LYP/HW\*/6-311+G(d,p) level where HW\* indicates that  $\text{Rb}^+$  and  $\text{Cs}^+$  were described using the effective core potentials (ECPs) and valence basis sets of Hay and Wadt<sup>25</sup> with a single d polarization function (exponents of 0.24 and 0.19, respectively) included.<sup>26</sup> Relative energies are determined using single point energies at the B3LYP, B3P86, and MP2(full) levels using the HW\*/6-311+G(2d,2p) basis set. In previous work on serine complexes,<sup>3</sup> similar HW\* calculations were performed for  $\text{K}^+(\text{Ser})$  complexes (with an exponent of 0.48 for the d polarization function on  $\text{K}^+$ ) in order to assess the accuracy of the Hay–Wadt ECP–valence basis sets. It was determined that vibrational frequencies calculated using the all-electron *vs.* HW\* basis sets on K yield results that differ by an average of less than 0.03%. Therefore, we did not perform HW\* calculations on  $\text{K}^+(\text{Met})$  complexes and conclude that the use of the HW\* basis sets for the  $\text{Rb}^+$  and  $\text{Cs}^+$  systems should yield equivalent results to the all-electron basis sets used for the smaller cations. In addition to using the HW\* basis sets on

Rb<sup>+</sup> and Cs<sup>+</sup> complexes, we also performed geometry optimizations, frequency calculations, and single point energy calculations using the Def2TZVP basis sets of triple- $\zeta$  valence quality for all elements.<sup>27</sup> These basis sets for Rb and Cs are designed to be used with small core ECPs developed by Leininger *et al.*<sup>28</sup>

Vibrational frequencies and intensities were calculated using the harmonic oscillator approximation and analytical derivatives of the energy-minimized Hessian calculated at the levels of theory noted above. Frequencies were scaled by 0.975 as this scaling factor leads to good agreement between calculated and experimentally well-resolved peaks and is in accord with previous IRMPD studies as well.<sup>6–8,29</sup> For comparison to experiment, calculated vibrational frequencies are broadened using a 20 cm<sup>-1</sup> fwhm Gaussian line shape.

## Results and discussion

### Theoretical results

The low-lying structures found for all M<sup>+</sup> (Met) complexes are illustrated by those for Rb<sup>+</sup> (Met) in Fig. 1. The nomenclature used to identify different structural isomers is identical to that described previously for the CID study of alkali-metal asparagine complexes<sup>6</sup> and differs somewhat from that utilized in the CID study of Met complexes.<sup>2</sup> Briefly, conformations of M<sup>+</sup> (Met) are identified by their metal binding site (or protonation site) in brackets, followed by a description of the methionine orientation by a series of five dihedral angles. These dihedral angles start with the carboxylic acid hydrogen atom (or analogous proton attached to the NH<sub>2</sub> group for zwitterionic structures) to define the H–O–C–C dihedral angle and proceeds along the molecule to the terminal methyl group of the amino acid side chain (O–C–C–C, C–C–C–C, C–C–C–S, and C–C–S–C). The dihedral angles are distinguished as *cis* (c, for angles between 0° and 50°), *gauche* (g, 50°–135°) and *trans* (t, 135°–180°). Previously, we designated the conformations somewhat less completely by designating the HOCO angle followed by the last three side-chain dihedrals, C–C–C–C, C–C–C–S, and C–C–S–C. In all cases, the HOCO and HOCC bond angles are the inverse of one another, *i.e.*, *c* versus *t*, and the last three dihedral angles are identical. Descriptions of these structures have been provided for the cases of M<sup>+</sup> = Li<sup>+</sup>, Na<sup>+</sup>, and K<sup>+</sup> previously,<sup>2</sup> and the ESI<sup>+</sup> describes the variations among all five alkali-metal cations in more detail.

Relative energies including zero-point energy (ZPE) corrections with respect to the ground state calculated at three different levels of theory are given in Table 1 for the M<sup>+</sup> (Met) complexes. Because the relative Gibbs free energies at 298 K may be more relevant in describing the experimental distributions, these values are also listed in Table 1 and used throughout the discussion below. The overall trends in relative Gibbs free energies at 298 K calculated at the MP2(full) level are shown in Fig. 2. Comparable figures for the relative Gibbs free energies at 298 K calculated at the B3LYP and B3P86 levels can be found in ESI<sup>+</sup>, Fig. S1. Conversion from 0 K bond energies to 298 K free energies is accomplished using the rigid rotor–harmonic oscillator approximation with rotational

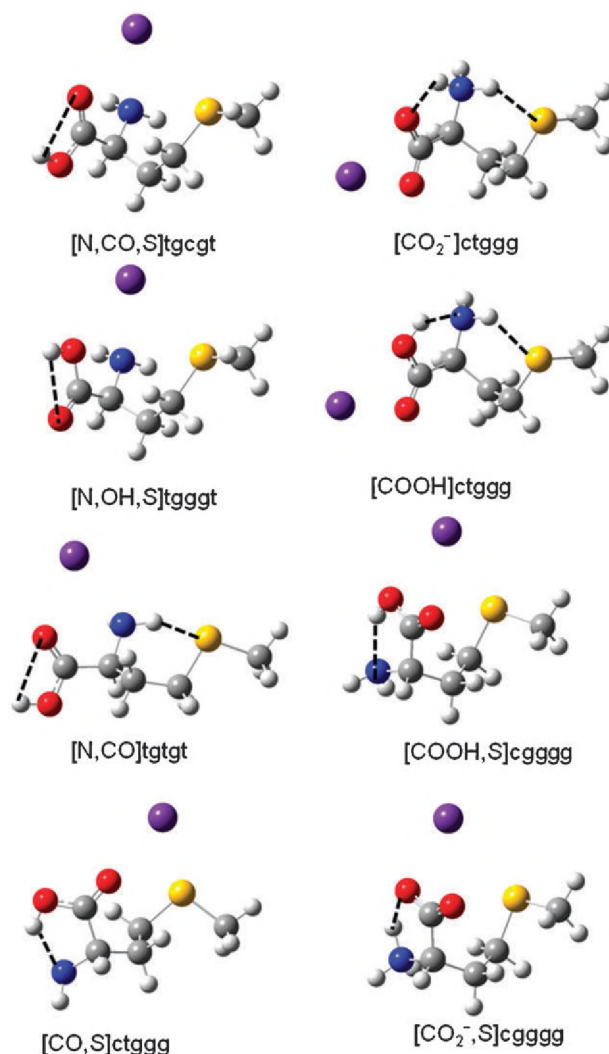
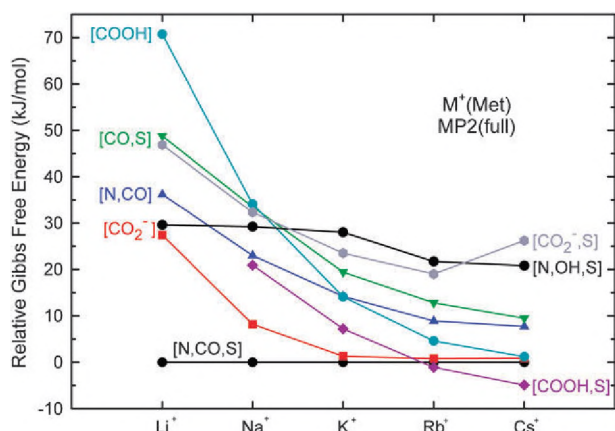


Fig. 1 Structures of the Rb<sup>+</sup>(Met) complexes calculated at the B3LYP/HW\*/6-311+G(d,p) level of theory. Hydrogen bonds are indicated by dashed lines.

constants and vibrational frequencies calculated at the B3LYP/6-311+G(d,p) and B3LYP/HW\*/6-311+G(d,p) levels. In the previous CID study of M<sup>+</sup> (Met) complexes,<sup>2</sup> three to four side-chain orientations were optimized for each distinct type of conformation, but only the lowest of these are plotted in Fig. 2. For the most part, the calculated IR spectra of the various side-chain orientations are very similar, such that a comparison with the lowest energy conformer is sufficient for identification; however, in the comparison between calculated and observed photodissociation spectra, spectral differences among these orientations will be discussed. Therefore, higher energy orientations that make up at least 1% of the ion population are included in Table 1. This corresponds to an excitation free energy of ~12 kJ mol<sup>-1</sup> above the ground state.

The charge-solvated, tridentate [N,CO,S] conformation is the lowest energy conformation for Li<sup>+</sup> (Met) and Na<sup>+</sup> (Met). For K<sup>+</sup> (Met), Rb<sup>+</sup> (Met), and Cs<sup>+</sup> (Met), the [N,CO,S] conformer is low-lying, 0–8, 1–10, and 5–13 kJ mol<sup>-1</sup>, respectively, higher in energy than the calculated ground state conformer.





**Fig. 2** 298 K Gibbs free energies ( $\text{kJ mol}^{-1}$ ) calculated at the MP2(full) level of theory (from Table 1) of eight conformations of  $M^+(\text{Met})$  complexes as a function of the alkali-metal cation relative to the energy of the  $[\text{N,CO,S}]$  conformer. The relative energy of the  $[\text{CO}_2^-]$  structure is higher than expected for  $\text{Cs}^+$  because the orientation preferred for  $\text{Li}^+$  to  $\text{Rb}^+$  collapses to a high energy  $[\text{CO}_2^-]$  structure.

The zwitterionic  $[\text{CO}_2^-]$  conformation lies  $>20 \text{ kJ mol}^{-1}$  higher than the  $[\text{N,CO,S}]$  ground state for  $\text{Li}^+(\text{Met})$ , however, as the metal cation becomes larger, the energetic difference between the  $[\text{N,CO,S}]$  and  $[\text{CO}_2^-]$  conformers decreases to 2–8  $\text{kJ mol}^{-1}$  at  $\text{Na}^+(\text{Met})$  and the two structures become nearly isoenergetic with one another at  $\text{K}^+(\text{Met})$  through  $\text{Cs}^+(\text{Met})$ , with excitation energies of 0–8, –1 to 10, and –1 to 13  $\text{kJ mol}^{-1}$ , respectively, Fig. 2. The  $[\text{COOH}]$  conformer, the charge-solvated analogue of the zwitterionic  $[\text{CO}_2^-]$  structure, starts 58–71  $\text{kJ mol}^{-1}$  higher than the ground state for  $\text{Li}^+(\text{Met})$ . As the metal cation becomes larger, the energy of the  $[\text{COOH}]$  conformer with respect to the ground state quickly decreases, but remains higher in energy than the  $[\text{CO}_2^-]$  conformation. For  $\text{Li}^+(\text{Met})$ , the  $[\text{CO}_2^-]$ – $[\text{COOH}]$  difference is 38–43  $\text{kJ mol}^{-1}$ , but decreases to 24–26, ~13, and ~4  $\text{kJ mol}^{-1}$  for  $M^+(\text{Met})$ ,  $M^+ = \text{Na}^+$ ,  $\text{K}^+$ , and  $\text{Rb}^+$ , respectively. For  $\text{Cs}^+(\text{Met})$ , the difference drops to 0.3–1.9  $\text{kJ mol}^{-1}$ . The charge-solvated, tridentate  $[\text{COOH,S}]$  conformation lies 19–23  $\text{kJ mol}^{-1}$  above  $[\text{N,CO,S}]$  at  $\text{Na}^+(\text{Met})$ . For  $\text{Li}^+(\text{Met})$ , this structure collapses to the bidentate  $[\text{CO,S}]$ . At the MP2 level of theory, the  $[\text{COOH,S}]$  conformer becomes the lowest energy state for  $\text{Rb}^+(\text{Met})$  and  $\text{Cs}^+(\text{Met})$ , lying 2 and 5  $\text{kJ mol}^{-1}$ , respectively, below  $[\text{CO}_2^-]$ , but the DFT calculations indicate the opposite order, with  $[\text{COOH,S}]$  lying 3–5 and 0–1  $\text{kJ mol}^{-1}$ , respectively, above  $[\text{CO}_2^-]$ . Overall, the 298 K free energies of the  $[\text{N,CO,S}]$ ,  $[\text{CO}_2^-]$ ,  $[\text{COOH}]$ , and  $[\text{COOH,S}]$  conformers all lie within 10 and 13  $\text{kJ mol}^{-1}$  of one another for  $\text{Rb}^+(\text{Met})$  and  $\text{Cs}^+(\text{Met})$ , respectively.

The  $[\text{CO}_2^-\text{,S}]$  conformer, the zwitterionic analogue of the charge-solvated  $[\text{COOH,S}]$  conformer, lies 11–14  $\text{kJ mol}^{-1}$  above the  $[\text{COOH,S}]$  structure for  $\text{Na}^+(\text{Met})$ ; however, as the metal cation becomes larger, the difference between these two tridentate structures increases eventually reaching a difference of 31–32  $\text{kJ mol}^{-1}$  at  $\text{Cs}^+(\text{Met})$ . The charge-solvated, tridentate  $[\text{N,OH,S}]$  conformer lies 30–35  $\text{kJ mol}^{-1}$  above the  $[\text{N,CO,S}]$  ground state for  $\text{Li}^+(\text{Met})$  and remains fairly high in energy, only getting to within 21–30  $\text{kJ mol}^{-1}$  of

the  $[\text{N,CO,S}]$  conformer for  $\text{Cs}^+(\text{Met})$ . The charge-solvated bidentate  $[\text{N,CO}]$  conformer is 27–36  $\text{kJ mol}^{-1}$  higher than the tridentate  $[\text{N,CO,S}]$  ground state at  $\text{Li}^+(\text{Met})$ , but the difference between these two types of complexes decreases with larger cations, differing by 1–8  $\text{kJ mol}^{-1}$  at  $\text{Cs}^+(\text{Met})$ . Similar behavior is also observed for the charge-solvated, bidentate  $[\text{CO,S}]$  structure.

The  $[\text{CO}_2^-]$  and  $[\text{COOH}]$  conformers differ only in the position of the hydrogen atom shared by the carboxylic acid and amino groups, which moves only by 0.88 Å for  $\text{Li}^+(\text{Met})$  to 0.75 Å for  $\text{Cs}^+(\text{Met})$  for the ctggg orientation. Therefore, we also located the transition states (TSs) between these conformers using the synchronous transit-guided quasi-newton (STQN) method<sup>30</sup> at the B3LYP/6-311+G(d,p) ( $M^+ = \text{Li}^+$ ,  $\text{Na}^+$ , and  $\text{K}^+$ ) and B3LYP/HW\*/6-311+G(d,p) ( $M^+ = \text{Rb}^+$  and  $\text{Cs}^+$ ) levels. Single point energies were calculated at the three levels listed above using the 6-311+G(2d,2p) basis set for  $M^+ = \text{Na}^+$  and  $\text{K}^+$  and HW\*/6-311+G(2d,2p) basis set for  $M^+ = \text{Rb}^+$  and  $\text{Cs}^+$ . 0 K energies for these TSs with ZPE corrections are 37–43, 18–24, 9–15, 3–7, and 1–5  $\text{kJ mol}^{-1}$  higher in energy than the  $[\text{CO}_2^-]$  ctggg conformers for  $M^+ = \text{Li}^+$ ,  $\text{Na}^+$ ,  $\text{K}^+$ ,  $\text{Rb}^+$ , and  $\text{Cs}^+$ , respectively. When compared to the energies of the  $[\text{COOH}]$  ctggg conformer, the TS is 3  $\text{kJ mol}^{-1}$  lower for  $M^+ = \text{Li}^+$ , 4–8  $\text{kJ mol}^{-1}$  lower for  $M^+ = \text{Na}^+$ , 2–7  $\text{kJ mol}^{-1}$  lower for  $M^+ = \text{K}^+$ , 4  $\text{kJ mol}^{-1}$  lower to 1  $\text{kJ mol}^{-1}$  higher for  $M^+ = \text{Rb}^+$ , and 2  $\text{kJ mol}^{-1}$  lower to 3  $\text{kJ mol}^{-1}$  higher for  $M^+ = \text{Cs}^+$ . Therefore, once ZPEs are included, the  $[\text{COOH}]$  ctggg conformer of  $\text{Li}^+(\text{Met})$ ,  $\text{Na}^+(\text{Met})$ , and  $\text{K}^+(\text{Met})$  collapses to the lower energy zwitterionic  $[\text{CO}_2^-]$  ctggg with no barrier to proton transfer, whereas for  $\text{Rb}^+(\text{Met})$  and  $\text{Cs}^+(\text{Met})$ , small barriers for proton transfer of ~1 and ~3  $\text{kJ mol}^{-1}$ , respectively, are calculated at the B3LYP and MP2(full) levels, but no barrier is found at the B3P86 level.

In order to more completely evaluate the utility of the HW\* basis sets for the heavier  $\text{Rb}^+$  and  $\text{Cs}^+$  metal cations, relative free energies at 298 K for their complexes with Met were also calculated utilizing the Def2TZVP basis sets at the B3LYP, B3P86, and MP2(full) levels of theory, Table 2. Relative 0 K energies utilizing the same basis set treatment are presented in ESI†, Table S1. Overall, the relative free energies using the Def2TZVP basis sets change very little compared to the results of the HW\*/6-311+G(2d,2p) basis set. For  $\text{Rb}^+(\text{Met})$ , DFT energies from both treatments agree that the  $[\text{CO}_2^-]$  conformer is the lowest energy structure. MP2(full) calculations using the HW\* and Def2TZVP basis sets predict that a  $[\text{COOH,S}]$  conformer is the lowest energy conformer. The MP2(full) energies using the HW\* basis set predict that the  $[\text{CO}_2^-]$ ,  $[\text{N,CO,S}]$ , and  $[\text{COOH,S}]$  conformers lie within 2  $\text{kJ mol}^{-1}$  of one another for HW\* and less than 0.5  $\text{kJ mol}^{-1}$  with the Def2TZVP basis set. For all basis sets,  $[\text{CO}_2^-]$ ,  $[\text{N,CO,S}]$ ,  $[\text{COOH}]$ , and  $[\text{COOH,S}]$  conformers lie within 10  $\text{kJ mol}^{-1}$  of one another.

For  $\text{Cs}^+(\text{Met})$ , the B3P86 level of theory with the HW\* basis set maintains that the  $[\text{CO}_2^-]$  structure is the lowest energy complex, whereas the B3LYP and MP2(full) levels of theory calculate a  $[\text{COOH,S}]$  conformer as the lowest energy state. Additionally, all levels of theory with the Def2TZVP basis set determine the  $[\text{COOH,S}]$  conformer to be the lowest

**Table 1** Relative energies at 0 K and free energies at 298 K (kJ mol<sup>-1</sup>) of low-lying conformers of cationized Met<sup>a</sup>

| Complex                                | Structure                              | B3LYP         | B3P86       | MP2(full)   |
|--|--|---------------|-------------|-------------|
| Li <sup>+</sup> (Met)                  | [N.CO.S]tgcgt                          | 0.0 (0.0)     | 0.0 (0.0)   | 0.0 (0.0)   |
|  | [N.CO.S]tgcgg                          | 6.1 (6.0)     | 6.3 (6.2)   | 5.2 (5.1)   |
|  | [N.CO.S]tgggt                          | 11.2 (10.8)   | 11.2 (10.8) | 11.6 (11.2) |
|  | [N.CO.S]tgggg                          | 12.9 (12.2)   | 12.9 (12.3) | 12.4 (11.7) |
|  | [CO <sub>2</sub> <sup>-</sup> ]ctggg   | 27.4 (24.5)   | 23.1 (20.2) | 30.3 (27.4) |
|  | [N.CO]tgtgt                            | 31.9 (28.1)   | 31.4 (27.5) | 40.0 (36.2) |
|  | [N.OH.S]tgggt                          | 33.5 (32.9)   | 35.6 (35.0) | 30.1 (29.6) |
|  | [CO.S]ctggg                            | 40.5 (37.3)   | 39.4 (36.2) | 52.0 (48.8) |
|  | [CO <sub>2</sub> <sup>-</sup> .S]cgggg | 52.2 (51.9)   | 48.6 (48.4) | 47.2 (46.9) |
|  | TS[CO <sub>2</sub> <sup>-</sup> .COOH] | 68.0 (64.5)   | 60.2 (56.7) | 73.0 (69.5) |
|  | [COOH]ctggg                            | 70.6 (65.4)   | 63.6 (58.5) | 75.8 (70.7) |
|  | [COOH.S]cgggg <sup>b</sup>             |               |             |             |
|  | Na <sup>+</sup> (Met)                  | [N.CO.S]tgcgt | 0.0 (0.0)   | 0.0 (0.0)   |
| [N.CO.S]tgcgg                          |  | 7.3 (7.1)     | 7.6 (7.4)   | 6.8 (6.6)   |
| [N.CO.S]tgggt                          |  | 8.7 (8.6)     | 8.6 (8.5)   | 8.1 (8.0)   |
| [CO <sub>2</sub> <sup>-</sup> ]ctggg   |  | 10.1 (7.7)    | 4.6 (2.3)   | 10.5 (8.2)  |
| [CO <sub>2</sub> <sup>-</sup> ]cgtgg   |  | 10.3 (7.9)    | 5.6 (3.2)   | 13.3 (10.9) |
| [N.CO.S]tgggg                          |  | 12.2 (11.9)   | 11.6 (11.3) | 9.4 (9.1)   |
| [CO <sub>2</sub> <sup>-</sup> ]ctggt   |  | 12.8 (10.3)   | 7.6 (5.1)   | 14.8 (12.3) |
| [N.CO]tgtgt                            |  | 23.3 (19.3)   | 21.8 (17.8) | 27.1 (23.0) |
| [COOH.S]cgcgg                          |  | 29.3 (23.4)   | 25.2 (19.3) | 26.8 (20.9) |
| [CO.S]ctggg                            |  | 29.3 (26.6)   | 26.8 (24.1) | 36.2 (33.5) |
| [N.OH.S]tgggt                          |  | 32.6 (31.8)   | 34.3 (33.5) | 29.9 (29.2) |
| TS[CO <sub>2</sub> <sup>-</sup> .COOH] |  | 33.3 (30.7)   | 23.0 (20.4) | 34.3 (31.7) |
| [COOH]ctggg                            |  | 37.8 (33.2)   | 31.0 (26.5) | 38.7 (34.1) |
| [CO <sub>2</sub> <sup>-</sup> .S]cgggg | 37.9 (37.3)                            | 33.6 (32.9)   | 32.9 (32.3) |             |
| K <sup>+</sup> (Met)                   | [CO <sub>2</sub> <sup>-</sup> ]ctggg   | 0.0 (0.0)     | 0.0 (0.0)   | 1.7 (1.3)   |
|  | [CO <sub>2</sub> <sup>-</sup> ]cgtgg   | 0.7 (0.4)     | 1.5 (1.2)   | 5.0 (4.2)   |
|  | [CO <sub>2</sub> <sup>-</sup> ]ctggt   | 2.6 (0.9)     | 2.8 (1.2)   | 5.5 (3.5)   |
|  | [N.CO.S]tgcgt                          | 2.7 (3.1)     | 7.8 (8.2)   | 0.0 (0.0)   |
|  | [N.CO.S]tgggt                          | 9.3 (9.9)     | 14.4 (15.0) | 5.4 (5.5)   |
|  | [N.CO.S]tgcgg                          | 10.1 (10.3)   | 15.3 (15.6) | 7.1 (7.0)   |
|  | [N.CO.S]tgggg                          | 10.8 (12.7)   | 14.8 (16.6) | 3.3 (4.7)   |
|  | [COOH.S]cgggt                          | 12.6 (11.1)   | 15.1 (13.5) | 10.0 (8.1)  |
|  | [COOH.S]cgcgg                          | 13.0 (13.1)   | 15.3 (15.4) | 8.5 (8.2)   |
|  | [COOH.S]cgggg                          | 13.1 (13.0)   | 15.1 (14.9) | 7.8 (7.2)   |
|  | TS[CO <sub>2</sub> <sup>-</sup> .COOH] | 13.5 (13.0)   | 9.4 (8.9)   | 15.2 (14.3) |
|  | [N.CO]tgtgt                            | 15.2 (12.2)   | 19.9 (16.8) | 17.6 (14.2) |
|  | [COOH]ctggg                            | 15.4 (12.6)   | 16.0 (13.2) | 17.3 (14.1) |
| [CO.S]ctggg                            | 18.1 (15.5)                            | 21.6 (19.0)   | 22.4 (19.4) |             |
| [CO <sub>2</sub> <sup>-</sup> .S]cgggg | 29.3 (28.6)                            | 30.2 (29.6)   | 24.6 (23.5) |             |
| [N.OH.S]tgggt                          | 34.1 (33.4)                            | 40.4 (39.7)   | 29.2 (28.0) |             |
| Rb <sup>+</sup> (Met)                  | [CO <sub>2</sub> <sup>-</sup> ]ctggg   | 0.0 (0.0)     | 0.0 (0.0)   | 1.7 (1.9)   |
|  | [CO <sub>2</sub> <sup>-</sup> ]cgtgg   | 0.9 (0.6)     | 1.8 (1.5)   | 5.3 (5.3)   |
|  | [CO <sub>2</sub> <sup>-</sup> ]ctggt   | 2.5 (1.6)     | 2.8 (1.9)   | 5.8 (5.1)   |
|  | [N.CO.S]tgcgt                          | 5.0 (4.9)     | 10.0 (9.9)  | 0.9 (1.1)   |
|  | [COOH]ctggg                            | 6.4 (3.4)     | 7.5 (4.5)   | 8.4 (5.7)   |
|  | [COOH]cgtgg                            | 6.5 (3.9)     | 7.8 (5.2)   | 10.6 (8.3)  |
|  | [COOH.S]cgggt                          | 6.6 (2.7)     | 9.1 (5.2)   | 3.9 (0.4)   |
|  | [COOH.S]cgcgg                          | 6.7 (5.7)     | 9.3 (8.3)   | 2.0 (1.3)   |
|  | [COOH.S]cgggg                          | 7.2 (5.6)     | 9.4 (7.8)   | 1.4 (0.0)   |
|  | TS[CO <sub>2</sub> <sup>-</sup> .COOH] | 7.4 (6.8)     | 3.3 (2.7)   | 8.8 (8.5)   |
|  | [COOH]ctggt                            | 9.2 (5.7)     | 10.5 (7.0)  | 12.8 (9.7)  |
|  | [N.CO.S]tgggg                          | 10.1 (11.7)   | 13.9 (15.5) | 0.0 (1.9)   |
|  | [N.CO.S]tgggt                          | 10.6 (10.7)   | 15.6 (15.7) | 4.5 (4.9)   |
| [N.CO.S]tgcgg                          | 12.3 (10.5)                            | 17.5 (15.7)   | 8.2 (6.7)   |             |
| [N.CO]tgtgt                            | 12.5 (8.8)                             | 17.4 (13.7)   | 13.3 (10.0) |             |
| [CO.S]ctggg                            | 13.0 (10.2)                            | 16.5 (13.7)   | 16.4 (13.9) |             |
| [CO <sub>2</sub> <sup>-</sup> .S]cgggg | 28.7 (24.8)                            | 29.1 (25.2)   | 23.7 (20.1) |             |
| [N.OH.S]tgggt                          | 34.0 (36.7)                            | 37.9 (40.5)   | 19.9 (22.8) |             |
| Cs <sup>+</sup> (Met)                  | [CO <sub>2</sub> <sup>-</sup> ]ctggg   | 0.0 (1.2)     | 0.0 (0.0)   | 3.2 (5.8)   |
|  | [CO <sub>2</sub> <sup>-</sup> ]cgtgg   | 1.1 (4.2)     | 1.8 (3.6)   | 7.6 (11.9)  |
|  | [COOH]cgtgg                            | 1.3 (1.6)     | 3.0 (2.1)   | 7.4 (9.0)   |
|  | [COOH]ctggg                            | 1.5 (1.6)     | 3.1 (1.9)   | 4.7 (6.1)   |
|  | [COOH.S]ctggt                          | 2.5 (0.0)     | 5.0 (1.3)   | 1.2 (0.0)   |
|  | [CO <sub>2</sub> <sup>-</sup> ]cgggt   | 2.8 (4.3)     | 3.1 (3.3)   | 7.6 (10.4)  |
|  | [COOH.S]cgcgg                          | 3.2 (4.7)     | 6.0 (6.3)   | 0.2 (3.0)   |
|  | [COOH]ctggt                            | 4.0 (1.9)     | 5.9 (2.5)   | 9.3 (8.4)   |
|  | [COOH.S]cgggg                          | 4.2 (4.8)     | 6.7 (6.0)   | 0.4 (2.4)   |
|  | TS[CO <sub>2</sub> <sup>-</sup> .COOH] | 4.7 (6.5)     | 0.7 (1.3)   | 7.7 (10.9)  |
|  | [N.CO.S]tgcgt                          | 7.2 (9.1)     | 12.2 (12.8) | 3.7 (7.0)   |

**Table 1** (continued)

| Complex              | Structure                              | B3LYP       | B3P86       | MP2(full)   |
|----------------------|--|-------------|-------------|-------------|
| H <sup>+</sup> (Met) | [N,CO,S]tgggg                          | 9.3 (12.9)  | 13.2 (15.6) | 0.0 (4.9)   |
|                      | [CO,S]ctgtg                            | 9.4 (9.2)   | 13.1 (11.7) | 15.3 (14.4) |
|                      | [N,CO]tgtgt                            | 11.0 (9.8)  | 16.2 (13.8) | 12.5 (12.6) |
|                      | [N,CO,S]tgggt                          | 11.6 (13.2) | 16.6 (16.9) | 6.3 (9.1)   |
|                      | [N,CO,S]tgcgg                          | 12.0 (10.4) | 16.9 (14.0) | 9.0 (8.7)   |
|                      | [CO <sub>2</sub> <sup>-</sup> ,S]cgcgg | 30.1 (32.2) | 31.1 (32.0) | 27.7 (31.1) |
|                      | [N,OH,S]ttggg                          | 32.9 (37.6) | 36.7 (40.1) | 19.8 (25.7) |
|                      | [N,CO,S]tgtgg                          | 0.0 (0.0)   | 0.0 (0.0)   | 0.0 (0.0)   |
|                      | [N,CO,S]tgggg                          | 2.6 (3.0)   | 2.0 (2.4)   | 0.4 (0.8)   |
|                      | [N,CO,S]tgtgt                          | 2.7 (1.9)   | 3.1 (2.3)   | 3.9 (3.1)   |
|                      | [N,CO,S]tgggt                          | 3.6 (3.3)   | 3.2 (2.9)   | 2.5 (2.2)   |
|                      | [N,OH,S]tgtgg                          | 15.4 (12.7) | 16.6 (13.9) | 14.5 (11.8) |
|                      | [N,OH,S]ttggg                          | 17.2 (17.4) | 17.7 (17.9) | 13.7 (13.9) |
|                      | [N,OH,S]tgtgt                          | 17.5 (13.9) | 19.2 (15.6) | 17.9 (14.2) |
| [N,OH,S]ttgtt        | 18.9 (17.9)                            | 19.8 (18.8) | 16.5 (15.5) |             |

<sup>a</sup> Free energies in parentheses. All values calculated at the level of theory indicated using the 6-311+G(2d,2p) basis set with structures and zero-point energies calculated at the B3LYP/6-311+G(d,p) level of theory. Values in italics use the HW\* basis set on the metal. <sup>b</sup> The [COOH,S] conformer for Li<sup>+</sup> (Met) collapses to [CO,S].

**Table 2** Relative free energies at 298 K (kJ mol<sup>-1</sup>) of low-lying conformations of cationized Met calculated using different basis sets<sup>a</sup>

| Complex                                | Structure                              | HW*/6-311+G(2d,2p)                   | Def2TZVP         |
|--|--|--------------------------------------|------------------|
| Rb <sup>+</sup> (Met)                  | [CO <sub>2</sub> <sup>-</sup> ]ctggg   | 0.0, 0.0, 1.9                        | 0.0, 0.0, 0.5    |
|  | [N,CO,S]tgcgt                          | 4.9, 9.9, 1.1                        | 2.5, 7.3, 0.2    |
|  | [COOH]ctggg                            | 3.4, 4.5, 5.7                        | 4.5, 5.3, 7.2    |
|  | [COOH,S]cgggt                          | 2.7, 5.2, 0.4                        | 4.1, 6.3, 0.0    |
|  | [COOH,S]cgggg                          | 5.6, 7.8, 0.0                        | 6.5, 8.4, 1.4    |
|  | [N,CO]tgtgt                            | 8.8, 13.7, 10.0                      | 7.8, 12.5, 11.1  |
|  | [CO,S]ctggg                            | 10.2, 13.7, 13.9                     | 9.4, 12.7, 13.7  |
|  | [CO <sub>2</sub> <sup>-</sup> ,S]cgggg | 24.8, 25.2, 20.1                     | 23.3, 23.3, 15.4 |
|  | [N,OH,S]ttggg                          | 36.7, 40.5, 22.8                     | 35.7, 39.6, 24.8 |
|  | Cs <sup>+</sup> (Met)                  | [CO <sub>2</sub> <sup>-</sup> ]ctggg | 1.2, 0.0, 5.8    |
| [COOH]ctggg                            |  | 1.6, 1.9, 6.1                        | 5.6, 4.8, 11.8   |
| [COOH,S]ctggt                          |  | 0.0, 1.3, 0.0                        | 0.0, 0.0, 0.0    |
| [N,CO,S]tgcgt                          |  | 9.1, 12.8, 7.0                       | 9.0, 11.3, 8.7   |
| [CO,S]ctgtg                            |  | 9.2, 11.7, 14.4                      | 11.6, 13.0, 18.0 |
| [N,CO]tgtgt                            |  | 9.8, 13.8, 12.6                      | 11.6, 14.3, 17.8 |
| [CO <sub>2</sub> <sup>-</sup> ,S]cgcgg |  | 32.2, 32.0, 31.1                     | 32.9, 31.3, 28.6 |
| [N,OH,S]ttggg                          |  | 37.6, 40.1, 25.7                     | 39.4, 40.9, 30.2 |

<sup>a</sup> Values listed are calculated at the B3LYP, B3P86, and MP2(full) levels of theory using the indicated basis set. For the Def2TZVP basis set on all elements, geometries and zero-point energies were calculated at the B3LYP/Def2TZVP level of theory.

energy structure. For both basis sets, all three levels of theory predict that the [N,CO,S] conformer lies 4–13 kJ mol<sup>-1</sup> above the lowest energy conformation. The [COOH] conformer lies 0–4 kJ mol<sup>-1</sup> above the [CO<sub>2</sub><sup>-</sup>] conformer at all levels of theory.

The vibrational frequencies calculated using the HW\*/6-311+G(d,p) and Def2TZVP basis sets are identical within about 2 cm<sup>-1</sup> for the Rb<sup>+</sup> (Met) and Cs<sup>+</sup> (Met) complexes. These results further indicate that the HW\*-calculations are adequate to describe relative energies and vibrational frequencies for the M<sup>+</sup> (Met) set of systems.

Finally, all levels of theory predict that the [N,CO,S] tgggt conformer is the lowest energy structure of the H<sup>+</sup> (Met) system, Table 1. Additional [N,CO,S] orientations lie within ~3 kJ mol<sup>-1</sup> of the tgtgg conformer. The [N,OH,S] analogues lie 11–16 kJ mol<sup>-1</sup> higher with respect to the analogous [N,CO,S] conformers at all levels of theory.

### IRMPD action spectroscopy

Photodissociation spectra of Met complexed with Li<sup>+</sup>, Na<sup>+</sup>, K<sup>+</sup>, Rb<sup>+</sup>, Cs<sup>+</sup>, and H<sup>+</sup> were examined. For the Na<sup>+</sup>, K<sup>+</sup>, Rb<sup>+</sup>, and Cs<sup>+</sup> complexes, photodissociation resulted in the loss of the intact ligand leaving the atomic metal cation. This result is consistent with collision-induced dissociation (CID) results for Na<sup>+</sup> (Met) and K<sup>+</sup> (Met).<sup>2</sup> For the complexes of K<sup>+</sup>, Rb<sup>+</sup>, and Cs<sup>+</sup>, Fig. 3 shows IRMPD action spectra taken from the relative intensity of the M<sup>+</sup> product cation as a function of laser wavelength. For Na<sup>+</sup> (Met), the results shown in Fig. 3 correspond to the depletion spectrum of the reactant complex as the Na<sup>+</sup> ion was difficult to collect in the FTICR and no other photodissociation products were observed for the Na<sup>+</sup> (Met) system. Because of these difficulties, the Na<sup>+</sup> (Met) spectrum only spans 900 to 1800 cm<sup>-1</sup>.

For Li<sup>+</sup> (Met), the CID spectra exhibit four low-energy channels corresponding to the loss of NH<sub>3</sub>, NH<sub>3</sub> + CO, C<sub>3</sub>H<sub>8</sub>S, and C<sub>3</sub>H<sub>8</sub>S + H<sub>2</sub>O.<sup>2</sup> The first two dissociation pathways were also observed in the IRMPD spectrum for Li<sup>+</sup> (Met) and have the greatest intensity upon photodissociation. Two additional channels consisting of the loss of H<sub>2</sub>O + CO and CH<sub>3</sub>SH were also observed in the IRMPD spectrum, but these decomposition pathways encompass less than 10% of the photodissociation signal. The sum of these four decomposition pathways is shown as the IRMPD action spectrum in Fig. 3. For most bands, loss of NH<sub>3</sub> (deamination) is 2–3 times more intense than the loss of NH<sub>3</sub> + CO, which is expected as deamination is the lowest energy decomposition pathway in the CID spectra of Li<sup>+</sup> (Met). However, these two dissociation pathways have the same intensity for bands at 1445 and 1595 cm<sup>-1</sup>.

For H<sup>+</sup> (Met), the IRMPD spectrum shown in Fig. 3 comprises the sum of the decomposition pathways corresponding to the loss of NH<sub>3</sub>, H<sub>2</sub>O + CO, H<sub>2</sub>O + CO + NH<sub>3</sub>, H<sub>2</sub>O + CO + CH<sub>3</sub>SH, and H<sub>2</sub>O + CO + NH<sub>3</sub> + C<sub>2</sub>H<sub>2</sub>. All of these decomposition pathways are consistent with observed products in the CID spectra of H<sup>+</sup> (Met) produced by electrospray ionization<sup>31</sup> and fast atom bombardment.<sup>32</sup> The deamination channel has about five times more intensity than the loss of H<sub>2</sub>O + CO throughout the spectrum. The latter three



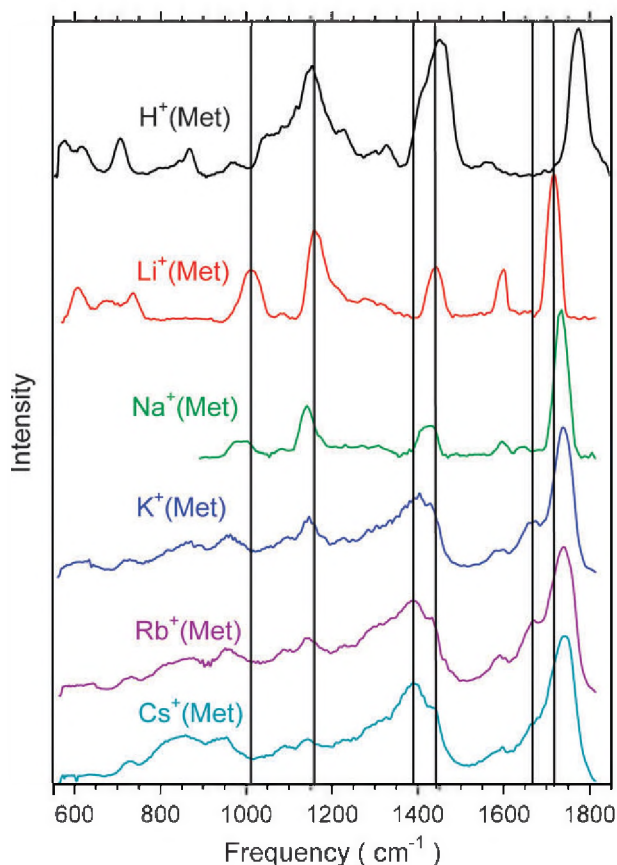


**Fig. 3** Infrared multiple photon dissociation action spectra of  $M^+(\text{Met})$  complexes, where  $M^+ = \text{Li}^+, \text{Na}^+, \text{K}^+, \text{Rb}^+, \text{Cs}^+, \text{and } \text{H}^+$ .

channels make up approximately 5% of the product intensities from photodissociation.

Comparison of the IRMPD spectra in Fig. 3 shows that the features observed in the  $\text{Li}^+(\text{Met})$  spectrum are retained for all of the metal cation complexes, but that new spectral features begin to appear for  $\text{K}^+(\text{Met})$ . The major band at  $1716 \text{ cm}^{-1}$  shifts to the blue as the metal cation becomes heavier and the bands at  $1160$  and  $1015 \text{ cm}^{-1}$  shift to the red. Spectral features at  $735$ ,  $1085$ , and  $1595 \text{ cm}^{-1}$  remain largely unchanged as the size of the metal ion increases. The band at  $1445 \text{ cm}^{-1}$  for  $\text{Li}^+(\text{Met})$  red shifts to  $1430 \text{ cm}^{-1}$  in  $\text{Na}^+(\text{Met})$ , and the photodissociation signal in this frequency range increases substantially for  $\text{K}^+(\text{Met})$ ,  $\text{Rb}^+(\text{Met})$ , and  $\text{Cs}^+(\text{Met})$ . A new band emerges at  $1670 \text{ cm}^{-1}$  for  $\text{K}^+(\text{Met})$  and  $\text{Rb}^+(\text{Met})$ , but is less distinct for  $\text{Cs}^+(\text{Met})$ . These progressions suggest multiple conformers are now present in the IRMPD spectra for the  $\text{K}^+$ ,  $\text{Rb}^+$ , and  $\text{Cs}^+$  complexes. Of considerable interest here is that the spectra for  $\text{K}^+(\text{Met})$ ,  $\text{Rb}^+(\text{Met})$ , and  $\text{Cs}^+(\text{Met})$  are virtually identical. In contrast, the IRMPD action spectrum for  $\text{H}^+(\text{Met})$  closely resembles a broadened version of the  $\text{Li}^+(\text{Met})$  spectrum, with the exception that the highest frequency band blue shifts to  $1770 \text{ cm}^{-1}$  and there is a distinct peak at  $865 \text{ cm}^{-1}$ .

#### Comparison of experimental and theoretical IR spectra: $\text{Li}^+(\text{Met})$

Fig. 4 shows the experimental IRMPD action spectrum along with calculated IR spectra for the seven distinct conformers of

$\text{Li}^+(\text{Met})$ . In making these comparisons, it should be remembered that the calculated IR intensities may not correspond exactly with the action spectrum because the latter is a multiple photon process, whereas the theoretical IR spectra are based on single photon absorption. Given this information, it is clear that the bands predicted by the  $[\text{N},\text{CO},\text{S}]$  conformer correspond well with the observed spectrum and have comparable relative intensities. All major bands are present with comparable theoretical and experimental frequencies. Alternative side-chain orientations of the  $[\text{N},\text{CO},\text{S}]$  conformer are sufficiently low in energy (Table 1) that they could also contribute to the experimental spectrum. According to the relative free energies in Table 1, the  $\text{tgccg}$  conformer could comprise 8–11% with the other two conformers contributing less than 2% presuming an equilibrium distribution at room temperature. The calculated frequencies for these higher energy structures are included in ESI†. No other distinct conformers are predicted to be low enough in energy to contribute to the experimental spectrum.

The band observed at  $1716 \text{ cm}^{-1}$  corresponds to the carbonyl stretch, which explains its large intensity. The CO stretch predicted by the  $[\text{N},\text{CO},\text{S}]\text{tgccg}$  conformer at  $1705 \text{ cm}^{-1}$  agrees with the observed band, but is red shifted by  $\sim 10 \text{ cm}^{-1}$ . The three higher energy  $[\text{N},\text{CO},\text{S}]$  conformers have comparable CO stretching frequencies at  $1708$  ( $\text{tgccg}$ ),  $1712$  ( $\text{tgccg}$ ), and  $1711$  ( $\text{tgccg}$ )  $\text{cm}^{-1}$ . Interaction with the lithium cation results in a red shift of this band with respect to free Met, calculated as  $1758$  and  $1782 \text{ cm}^{-1}$  depending on the specific conformation. The observed band at  $1595 \text{ cm}^{-1}$  has the largest deviation with the calculated spectra for the  $[\text{N},\text{CO},\text{S}]\text{tgccg}$  conformer, which has a band predicted at  $1624 \text{ cm}^{-1}$  (a frequency essentially invariant for the other orientations). This band describes the bending motion of the  $\text{NH}_2$  group and its predicted position is largely unaffected compared to  $\sim 1627 \text{ cm}^{-1}$  band for neutral Met. Such deviations between experiment and theory have been observed for  $\text{NH}_2$  bending modes in other systems<sup>3,4,33,34</sup> and are believed to result from strong anharmonic effects. The peaks observed at  $1445$ ,  $1160$ ,  $1015$ ,  $740$ ,  $680$ , and  $610 \text{ cm}^{-1}$  are well represented by the spectra calculated for the  $[\text{N},\text{CO},\text{S}]$  conformer. The band at  $1445 \text{ cm}^{-1}$  is a conglomerate of vibrations corresponding to HCH bends in the amino acid side chain. The band at  $1160 \text{ cm}^{-1}$  is primarily associated with bending of the H–O–C angle of the carboxylic acid moiety. This is one of the few bands where the spectra of the various  $[\text{N},\text{CO},\text{S}]$  conformers differ somewhat. The observed band corresponds particularly well with the calculated ground state  $\text{tgccg}$  conformer, as this has the most intensity at  $1163 \text{ cm}^{-1}$  with a shoulder at  $1183 \text{ cm}^{-1}$ . The shape of the band predicted for the  $\text{tgccg}$  conformer is also similar to the observed spectra with a strong band at  $1163$  and shoulder at  $1186 \text{ cm}^{-1}$ . The  $\text{tgccg}$  orientation has a single strong band at  $1173 \text{ cm}^{-1}$  with a shoulder at  $1148 \text{ cm}^{-1}$  and the  $\text{tgccg}$  orientation has two bands of equal intensity at  $1164$  and  $1174 \text{ cm}^{-1}$ . The profiles of these latter two bands do not agree as well with the observed spectrum, consistent with them making only small contributions to the observed spectrum. The  $[\text{N},\text{CO},\text{S}]$  spectra have predicted bands at  $1021$ – $1033 \text{ cm}^{-1}$ , the  $\text{NH}_2$  wagging motion, which is slightly blue shifted with respect to an observed peak

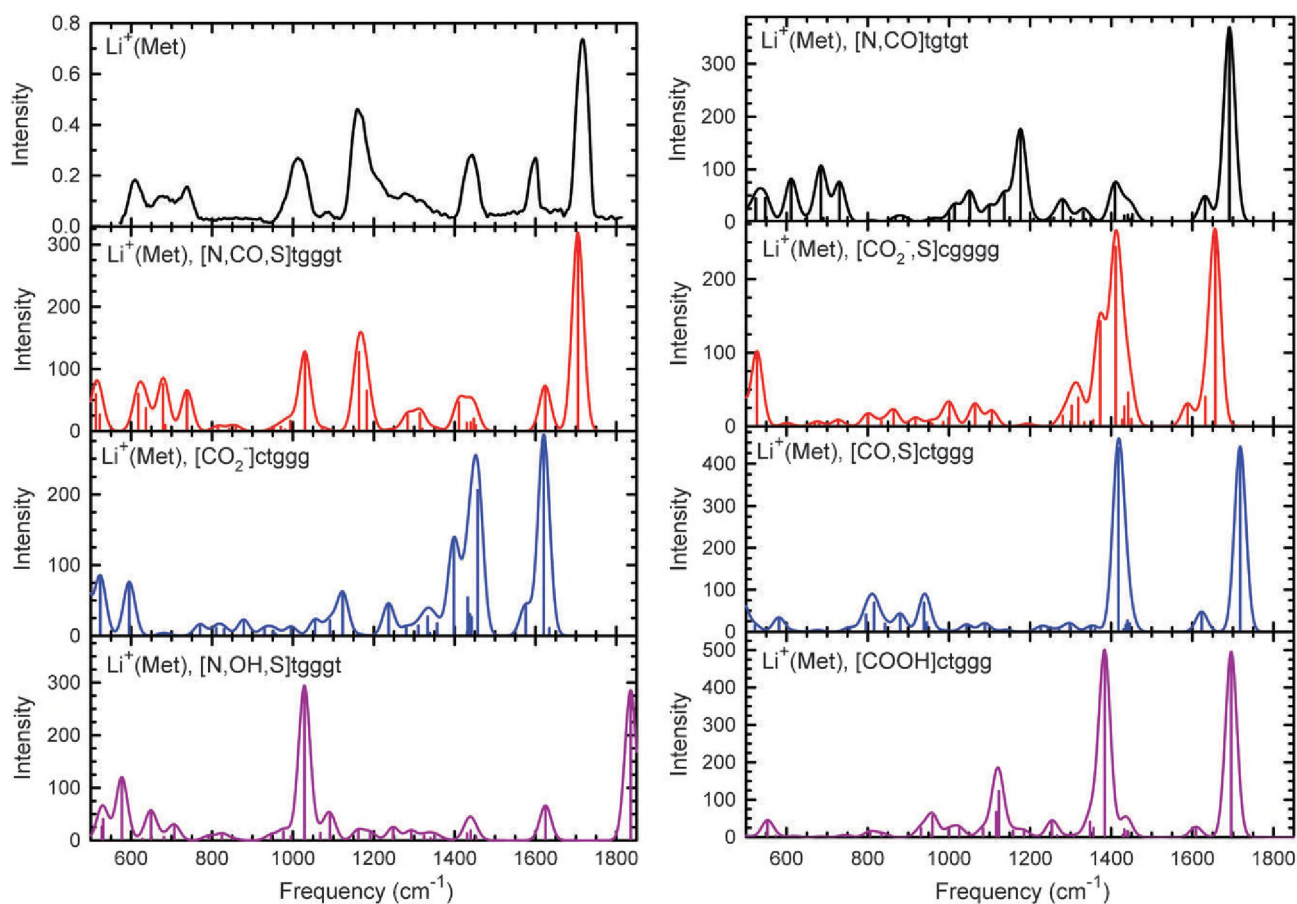


**Fig. 4** Comparison of the experimental IRMPD action spectrum for  $\text{Li}^+(\text{Met})$  with IR spectra predicted at the B3LYP/6-311+G(d,p) level of theory for seven conformations.

at  $1015\text{ cm}^{-1}$ . Observed peaks at  $610$ ,  $680$ , and  $740\text{ cm}^{-1}$  correspond to wagging motions of the carboxylic acid hydrogen atom and match the predicted spectra for all [N,CO,S] conformers well. Broad and weak bands observed at  $800\text{--}900\text{ cm}^{-1}$  and  $1250\text{--}1350\text{ cm}^{-1}$  are also consistent with predicted bands in the [N,CO,S] spectra. Finally, there is a weak band observed at  $1080\text{ cm}^{-1}$  that could correspond to a weak band in the [N,CO,S] calculated spectra associated with synchronous C–C and C–N bond stretches.

It is quite clear that the observed spectrum for  $\text{Li}^+(\text{Met})$  does not include any contributions from the zwitterionic  $[\text{CO}_2^-]$  and  $[\text{CO}_2^-\text{S}]$  conformers. The intense carbonyl stretch predicted at  $1620$  and  $1656\text{ cm}^{-1}$ , respectively, is much lower in frequency compared to free Met and the observed spectrum. Additionally, the broad bands at  $1250\text{--}1500\text{ cm}^{-1}$  in the predicted zwitterionic spectra are inconsistent with the experimental spectrum. There does not appear to be any contribution from the [N,OH,S] tggt conformer either. Compared to the [N,CO,S] calculated spectrum, this conformation has minimal diagnostic bands. The CO stretch ( $1835\text{ cm}^{-1}$ ) is considerably blue shifted with respect to the observed band at  $1716\text{ cm}^{-1}$ , but lies beyond the frequency range for the experimental spectrum. The major band predicted at  $1029\text{ cm}^{-1}$  overlaps with the predicted band at  $1030\text{ cm}^{-1}$  in the [N,CO,S] spectrum. Therefore, the bands at  $577$ ,  $649$ , and  $707\text{ cm}^{-1}$  corresponding to the wagging motion of the acid hydrogen atom are the most

diagnostic bands and do not match the observed spectrum. Although the predicted spectrum for the [N,CO] tgtgt conformer has a number of similarities to that for [N,CO,S] tggt, we can dismiss any contribution from the [N,CO] tgtgt conformation for  $\text{Li}^+(\text{Met})$ . First, the carbonyl stretch of the bidentate conformation ( $1690\text{ cm}^{-1}$ ) is red shifted with respect to the observed band at  $1716\text{ cm}^{-1}$  and calculated frequency of  $1705\text{--}1712\text{ cm}^{-1}$  in the [N,CO,S] conformation. Second, the predicted spectrum shows a low frequency shoulder for the band at  $1160\text{ cm}^{-1}$ , which is not observed. Finally, the predicted profile for the observed band at  $1015\text{ cm}^{-1}$  matches that predicted for the  $\text{NH}_2$  wagging motion in the [N,CO,S] tggt and tggg conformations at  $1030\text{--}1033\text{ cm}^{-1}$ , with a weaker low frequency shoulder and a steep profile at higher frequencies, in contrast to the relative intensities of these bands in the [N,CO] tgtgt spectrum. Similarly, the [CO,S] and [COOH] spectra do not reproduce the experimental spectrum with any fidelity. Overall, the experimental IRMPD action spectrum can be explained completely by the calculated spectra of the ground state [N,CO,S] tggt and tggg conformers.

#### Comparison of experimental and theoretical IR spectra: $\text{Na}^+(\text{Met})$

The  $\text{Na}^+(\text{Met})$  spectrum is very similar to the  $\text{Li}^+(\text{Met})$  spectrum over the available range of  $900$  to  $1800\text{ cm}^{-1}$ ,



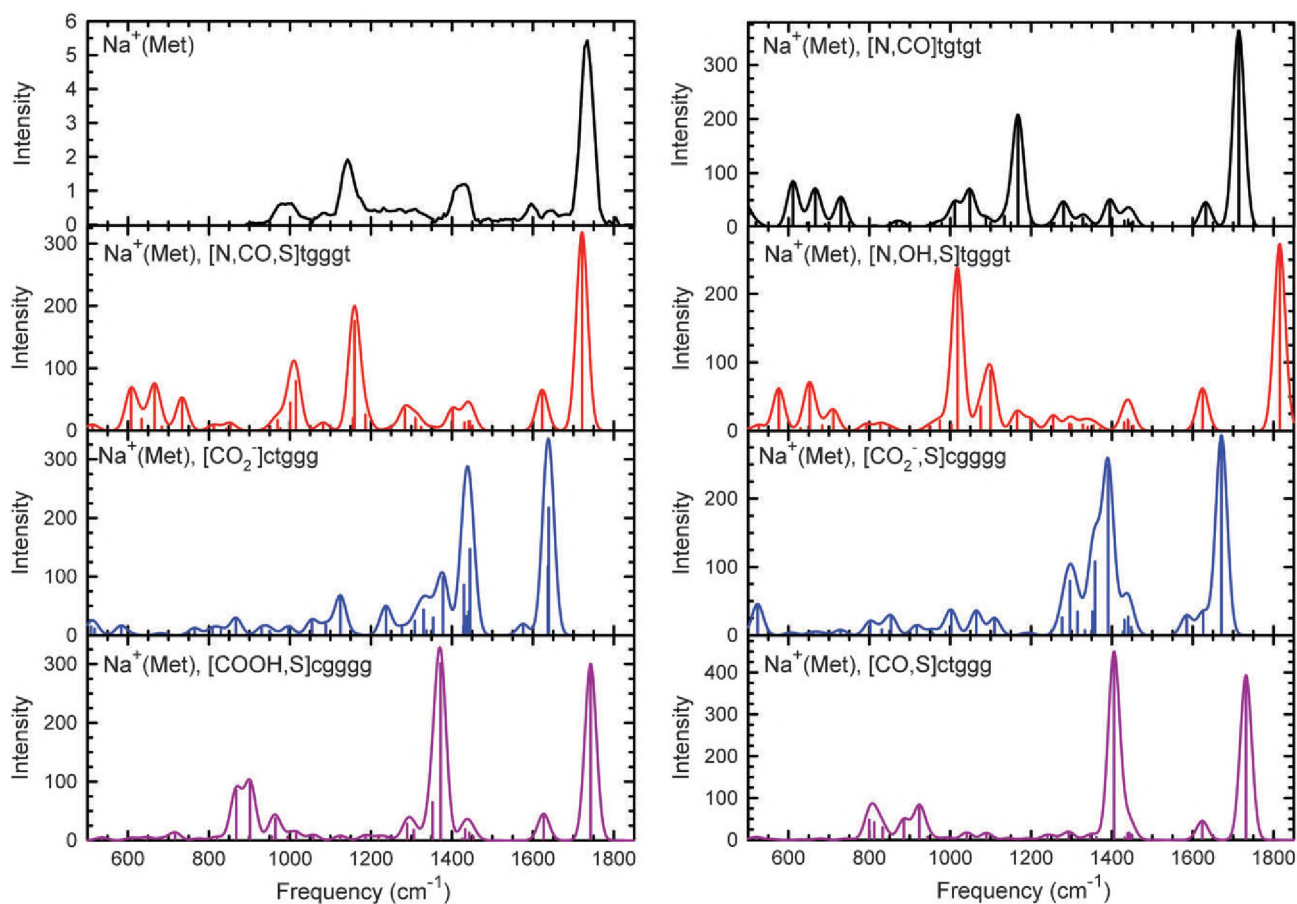


Fig. 5 Comparison of the experimental IRMPD action spectrum for  $\text{Na}^+(\text{Met})$  with IR spectra predicted at the B3LYP/6-311+G(d,p) level of theory for seven conformations.

Fig. 3. Subtle differences with respect to the action spectrum of  $\text{Li}^+(\text{Met})$  are present and include a blue shift in the band at  $1716\text{ cm}^{-1}$  to  $1734\text{ cm}^{-1}$  and bands that red shift from  $1015\text{ cm}^{-1}$  to  $1000\text{ cm}^{-1}$ ,  $1160\text{ cm}^{-1}$  to  $1140\text{ cm}^{-1}$ , and  $1445\text{ cm}^{-1}$  to  $1430\text{ cm}^{-1}$ . Bands located at  $1080$  and  $1595\text{ cm}^{-1}$  are unaffected. Comparison of the experimental spectrum with the theoretical spectra for  $\text{Na}^+(\text{Met})$  is shown in Fig. 5. As for  $\text{Li}^+(\text{Met})$ , the predicted  $[\text{N},\text{CO},\text{S}]$  tggtt spectrum shows a close correspondence to the limited observed spectrum for  $\text{Na}^+(\text{Met})$ . Notably, the predicted carbonyl stretch frequency shifts to higher frequency by  $16\text{ cm}^{-1}$  from  $\text{Li}^+(\text{Met})$  to  $\text{Na}^+(\text{Met})$ , in agreement with the experimental observation. Likewise the  $\text{NH}_2$  bending band at  $1595\text{ cm}^{-1}$  is predicted not to shift from  $\text{Li}^+(\text{Met})$  to  $\text{Na}^+(\text{Met})$ , consistent with experiment. Overall, the predicted spectra for the  $[\text{N},\text{CO},\text{S}]$  conformers of  $\text{Li}^+(\text{Met})$  and  $\text{Na}^+(\text{Met})$  accurately represent the changes observed with metal cation identity.

The major peaks observed in the  $\text{Na}^+(\text{Met})$  depletion spectrum at  $1735$ ,  $1430$ ,  $1140$ , and  $1000\text{ cm}^{-1}$  were also observed in the  $\text{Na}^+$  product ion spectrum (not shown); however, the weak bands observed at  $1650$ ,  $1595$ , and  $1080\text{ cm}^{-1}$  in the depletion spectrum were not present in the  $\text{Na}^+$  product ion spectrum. The weak band at  $1650\text{ cm}^{-1}$  cannot be described by the  $[\text{N},\text{CO},\text{S}]$  tggtt conformer, but could correspond to the carbonyl stretch (really an antisymmetric carboxylate stretch) for the zwitterionic  $[\text{CO}_2^-]$  ctggg and cgtgg

conformers calculated to lie at  $1639\text{ cm}^{-1}$ . It is possible that the experimental spectrum could contain the  $[\text{CO}_2^-]$  ctggg and cgtgg conformers, which are calculated to lie  $2\text{--}11\text{ kJ mol}^{-1}$  above the  $[\text{N},\text{CO},\text{S}]$  tggtt ground state, Table 1. One might anticipate that the presence of the  $[\text{CO}_2^-]$  conformer would also lead to a signal increase near  $1440\text{ cm}^{-1}$ ; however, the low intensity of the  $1650\text{ cm}^{-1}$  band suggests that this would be hidden by the spectral features already present from  $[\text{N},\text{CO},\text{S}]$ . If the relative intensities of the bands at  $1734$  and  $1650\text{ cm}^{-1}$  are reliable indicators of the relative populations of the two conformers (and this may not be the case for the reasons noted above), then the  $[\text{CO}_2^-]$  conformer would represent  $\sim 7\%$  of the signal present (consistent with an excitation energy of  $6.4\text{ kJ mol}^{-1}$  at  $298\text{ K}$ ).

#### Comparison of experimental and theoretical IR spectra: $\text{K}^+(\text{Met})$ and $\text{Rb}^+(\text{Met})$

Fig. 6 and 7 show the experimental IRMPD action spectrum of  $\text{K}^+(\text{Met})$  and  $\text{Rb}^+(\text{Met})$  compared with theoretical predictions for the seven lowest energy distinct conformations. Compared to the experimental spectra for  $\text{Li}^+(\text{Met})$  and  $\text{Na}^+(\text{Met})$ , the IRMPD spectrum of  $\text{K}^+(\text{Met})$  retains the same bands, but new features are present, Fig. 3. The spectrum for  $\text{Rb}^+(\text{Met})$  is very similar to that for  $\text{K}^+(\text{Met})$ , having the same number of new bands compared to the  $\text{Li}^+(\text{Met})$  and

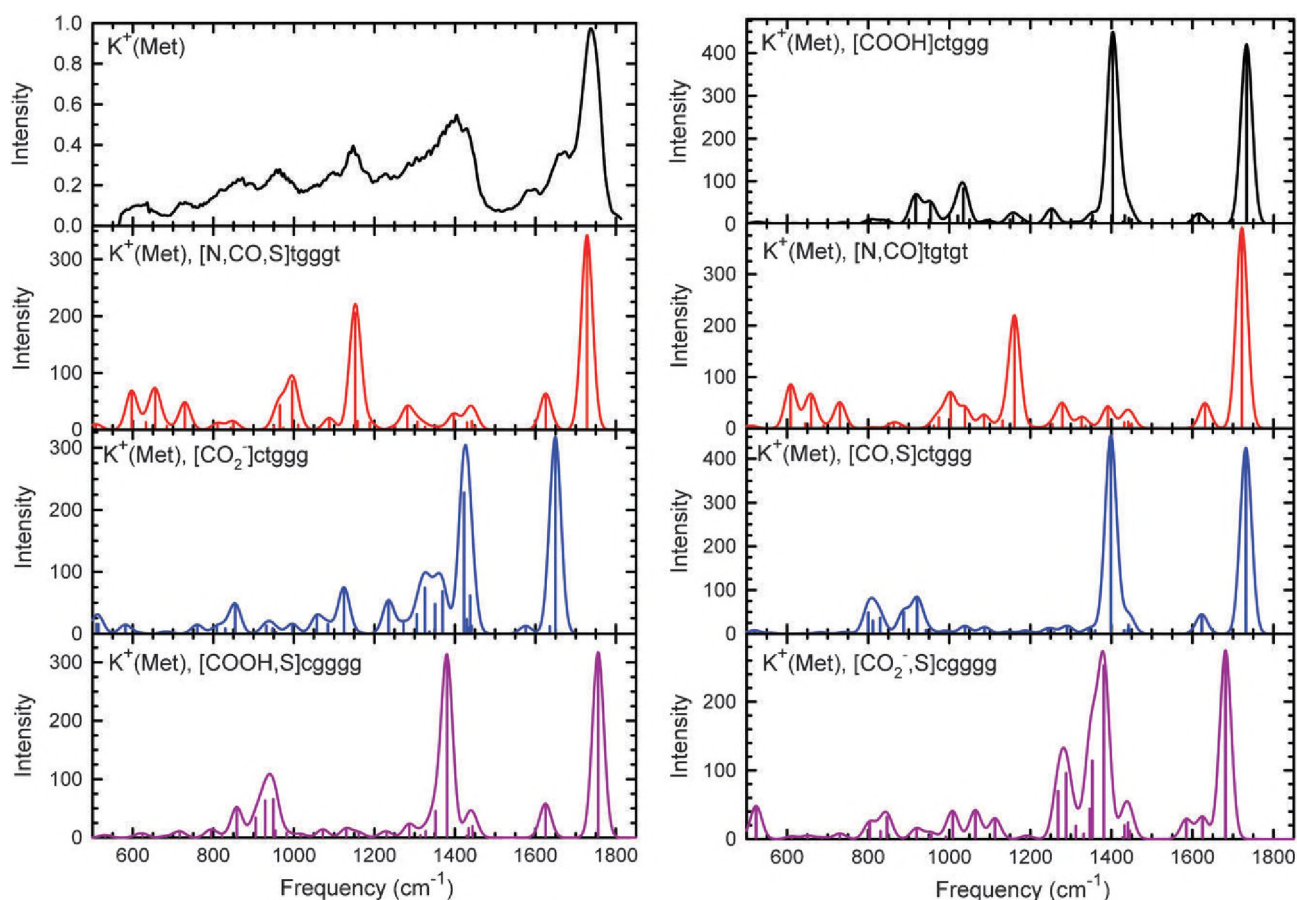


**Fig. 6** Comparison of the experimental IRMPD action spectrum for  $K^+(\text{Met})$  with IR spectra predicted at the B3LYP/6-311+G(d,p) level of theory for seven conformations.

$\text{Na}^+(\text{Met})$  spectra. These new bands could be attributed to new conformers present or could be attributed to improved sensitivity by more facile dissociation from this weakly bound system. However, in no case do the new experimental bands correspond to previously unobserved peaks in the predicted spectrum for [N,CO,S]. Hence, there is no indication that enhanced sensitivity can explain the new features.

New bands in the observed spectrum of  $K^+(\text{Met})$  [ $\text{Rb}^+(\text{Met})$ ] occur at 875 [880], 960 [955], 1225 [1230], 1405 [1395], and 1670 [1670]  $\text{cm}^{-1}$ . The band at 1430 [1430]  $\text{cm}^{-1}$  has grown in intensity with respect to  $\text{Na}^+(\text{Met})$  and a broad low frequency shoulder is now present. Overall, a comparison between the  $K^+(\text{Met})$  and  $\text{Rb}^+(\text{Met})$  spectra with those of  $\text{Li}^+(\text{Met})$  and  $\text{Na}^+(\text{Met})$  shows a considerable increase in photodissociation in the region from 750 to 1400  $\text{cm}^{-1}$ . The [N,CO,S] conformers may still be present as the predicted carbonyl stretch of 1724–1730 [1731–1737]  $\text{cm}^{-1}$  agrees well with the corresponding band observed at 1735 [1742]  $\text{cm}^{-1}$ ; however, carbonyl stretches of the [COOH] (1733 [1743]  $\text{cm}^{-1}$ ) and [CO,S] (1732 [1739]  $\text{cm}^{-1}$ ) conformers are equally consistent. The frequencies for the bending mode of the  $\text{NH}_2$  group in the [N,CO,S] spectra (1618–1626 [1618–1624]  $\text{cm}^{-1}$ ) are still blue shifted by  $\sim 30$   $\text{cm}^{-1}$  with respect to the observed band at  $\sim 1595$  [1590]  $\text{cm}^{-1}$ , consistent with observations for  $\text{Li}^+(\text{Met})$  and  $\text{Na}^+(\text{Met})$ . The intense calculated band at 1149–1152 [1143–1148]  $\text{cm}^{-1}$  corresponding to the C–O–H

bending mode of the [N,CO,S] conformer matches the observed spectrum for  $K^+(\text{Met})$  [ $\text{Rb}^+(\text{Met})$ ] well. Likewise, the wagging motions of the acidic hydrogen atom at 730 [735] and below 700  $\text{cm}^{-1}$  in the observed  $K^+(\text{Met})$  [ $\text{Rb}^+(\text{Met})$ ] spectrum are also well characterized in the calculated spectra for the [N,CO,S] conformer. These bands demonstrate the presence of the [N,CO,S] conformer as it and the higher energy [N,CO] are the only conformers with bands in this frequency range. Bands observed at 960 [955], 1100 [1090], and the shoulder at 1430 [1430]  $\text{cm}^{-1}$  could also have contributions from the [N,CO,S] conformer.

A prominent new peak at 1670 [1670]  $\text{cm}^{-1}$  in the observed spectra for  $K^+(\text{Met})$  [ $\text{Rb}^+(\text{Met})$ ] indicates the presence of the zwitterionic  $[\text{CO}_2^-]$  conformer. Calculated spectra for these conformers indicate this band appears at 1649–1650 [1660–1661]  $\text{cm}^{-1}$  for  $K^+(\text{Met})$  [ $\text{Rb}^+(\text{Met})$ ]. The appearance of this new peak is accompanied by the band observed at 1405 [1395]  $\text{cm}^{-1}$  along with a broad shoulder to the red. These new bands can be attributed to the intense band calculated at 1417–1423 [1408–1413]  $\text{cm}^{-1}$  in the predicted spectra for the three  $[\text{CO}_2^-]$  conformers along with several bands extending from 1225 [1230] to 1405 [1395]  $\text{cm}^{-1}$ . Bands observed at 875 [880] and 1100 [1090]  $\text{cm}^{-1}$  can also be described by bands calculated in all  $[\text{CO}_2^-]$  spectra.

Overall, the experimental spectra for  $K^+(\text{Met})$  and  $\text{Rb}^+(\text{Met})$  are adequately represented by contributions from



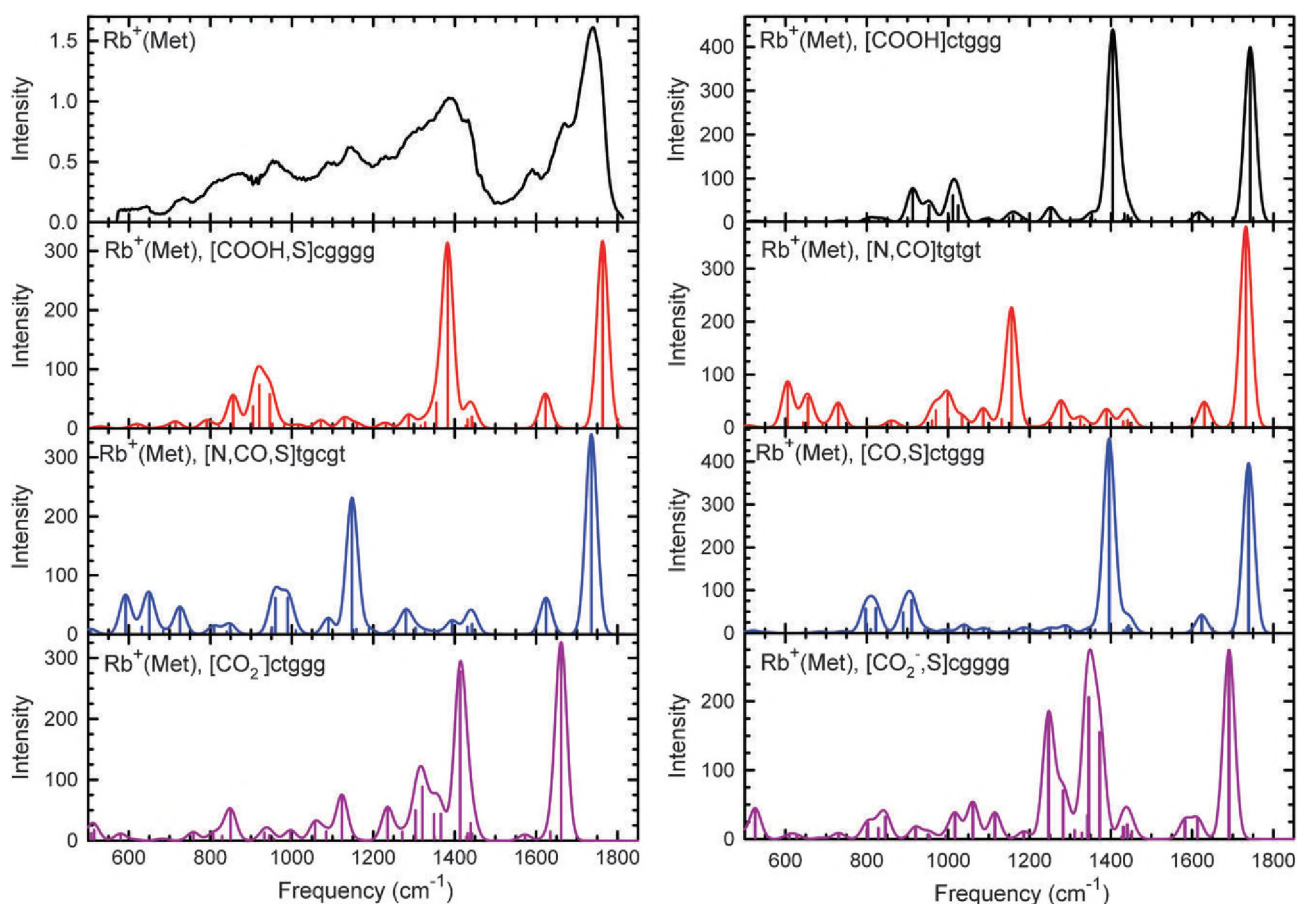


Fig. 7 Comparison of the experimental IRMPD action spectrum for  $\text{Rb}^+(\text{Met})$  with IR spectra predicted at the B3LYP/6-311+G(d,p) level of theory for seven conformations.

the  $[\text{N,CO,S}]$  and  $[\text{CO}_2^-]$  conformers. This is consistent with calculations for  $\text{K}^+(\text{Met})$ , which indicate that any other conformers lie at least  $7 \text{ kJ mol}^{-1}$  higher in energy, Table 1. Thus, at 298 K, contributions from  $[\text{COOH,S}]$  conformations are calculated to be  $< 6\%$  and those for any other conformer are  $< 1\%$ . For  $\text{Rb}^+(\text{Met})$ , both the  $[\text{COOH,S}]$  and  $[\text{COOH}]$  conformers lie low enough in energy ( $0\text{--}8$  and  $3\text{--}10 \text{ kJ mol}^{-1}$ , respectively, Table 1) to potentially contribute to the ion population. Indeed, the broad band observed at  $1405$  [ $1395$ ]  $\text{cm}^{-1}$  for  $\text{K}^+(\text{Met})$  [ $\text{Rb}^+(\text{Met})$ ] could have contributions from the intense bands at  $1378\text{--}1386$  [ $1374\text{--}1389$ ]  $\text{cm}^{-1}$  for the  $[\text{COOH,S}]$  conformers, which are attributed to the C–O–H bending mode. The relative intensities of the peaks observed at  $875$  [ $880$ ] and  $960$  [ $955$ ]  $\text{cm}^{-1}$  are also consistent with similar bands in the calculated spectra of the  $[\text{COOH,S}]$  cgggg and cgggt conformations, but notably not of the highest energy cggg orientation. Discounting the presence of the  $[\text{COOH,S}]$  conformers is the fact that the calculated carbonyl stretches ( $1750\text{--}1756$  [ $1756\text{--}1763$ ]  $\text{cm}^{-1}$ ) are blue shifted by  $15\text{--}20 \text{ cm}^{-1}$  with respect to the observed band at  $1735$  [ $1742$ ]  $\text{cm}^{-1}$ , in contrast to the red shift of  $\sim 15 \text{ cm}^{-1}$  observed for this band in the  $\text{Li}^+(\text{Met})$  and  $\text{Na}^+(\text{Met})$  spectra. There are no high frequency shoulders in this region of the observed spectra that would be consistent with the presence of considerable amounts of both the  $[\text{N,CO,S}]$  and  $[\text{COOH,S}]$  conformers, although minor amounts of the latter would lead to simple broadening

of this peak, which is possibly consistent with the data. In contrast, the carbonyl stretches at  $1733\text{--}1735$  [ $1743\text{--}1745$ ]  $\text{cm}^{-1}$  for the  $[\text{COOH}]$  conformers agree well with the CO stretch observed in the IRMPD spectra and would simply overlap the contribution from the  $[\text{N,CO,S}]$  conformer present. These three  $[\text{COOH}]$  conformers lie within  $4 \text{ kJ mol}^{-1}$  of one another for  $\text{K}^+(\text{Met})$  and  $\text{Rb}^+(\text{Met})$ , Table 1. These conformers also have an intense peak predicted at  $1403$  [ $1404\text{--}1410$ ]  $\text{cm}^{-1}$  that could correspond to the observed peak at  $1405$  [ $1395$ ]  $\text{cm}^{-1}$ . The  $[\text{COOH}]$  conformer has no additional distinctive bands that allow its presence to be verified. In conclusion, we can confidently attribute the observed spectra of  $\text{K}^+(\text{Met})$  and  $\text{Rb}^+(\text{Met})$  to dissociation from  $[\text{N,CO,S}]$  and  $[\text{CO}_2^-]$  conformers, but cannot rule out contributions from  $[\text{COOH,S}]$  and  $[\text{COOH}]$  conformers.

#### Comparison of experimental and theoretical IR spectra: $\text{Cs}^+(\text{Met})$

Fig. 8 shows the IRMPD action spectrum of  $\text{Cs}^+(\text{Met})$  with theoretical predictions for seven low-energy distinct conformers. All of the spectral features for  $\text{K}^+(\text{Met})$  and  $\text{Rb}^+(\text{Met})$  are still present in the  $\text{Cs}^+(\text{Met})$  spectrum, Fig. 3, with the only differences being increases in relative intensity between  $700\text{--}900$  and  $1200\text{--}1400 \text{ cm}^{-1}$ . Therefore, all of the comparisons between the observed spectrum and the predicted



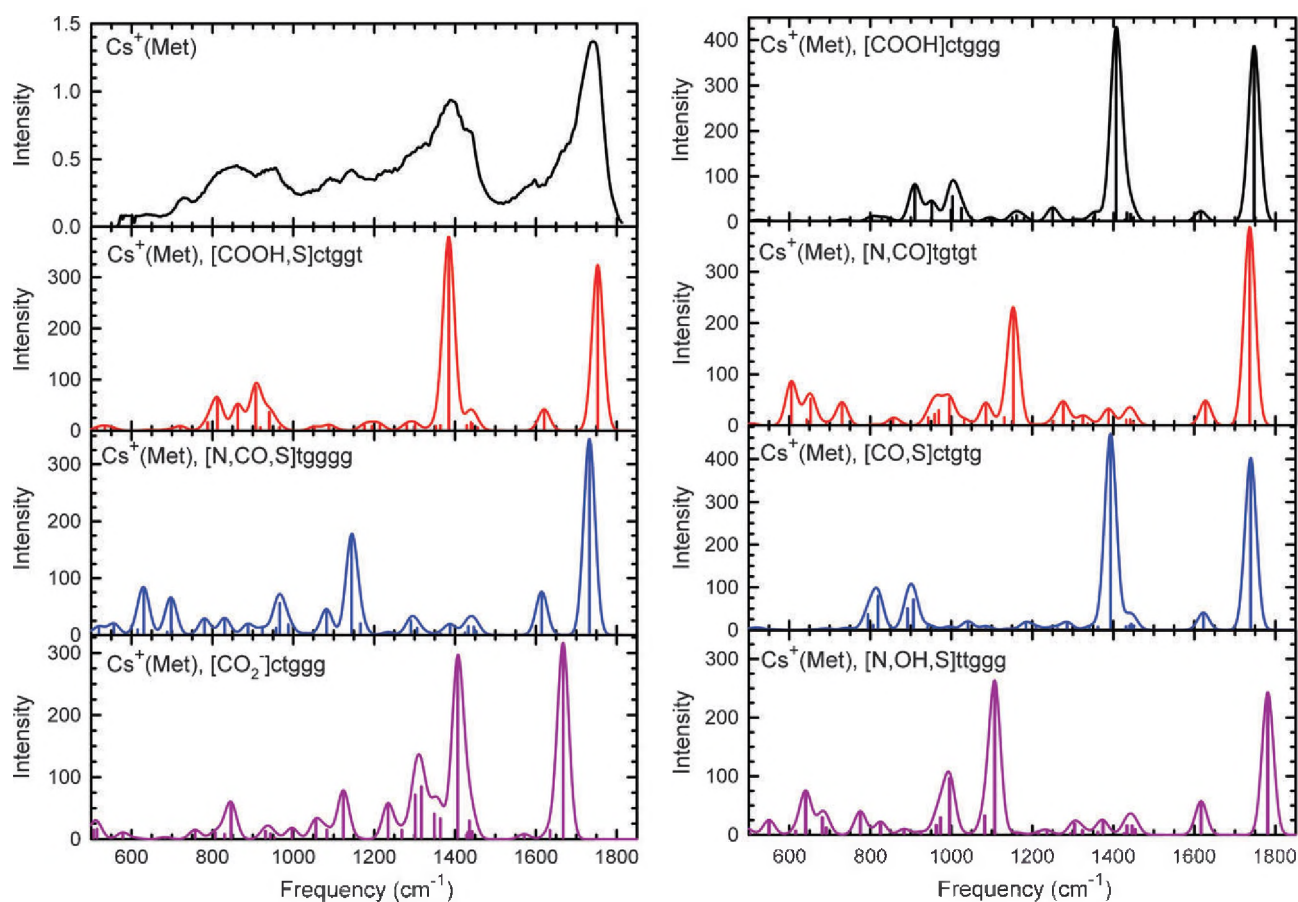


**Fig. 8** Comparison of the experimental IRMPD action spectrum for  $\text{Cs}^+(\text{Met})$  with IR spectra predicted at the B3LYP/HW\*/6-311+G(d,p) level of theory for seven conformations.

spectra mentioned in the previous section are still viable. Both  $[\text{N},\text{CO},\text{S}] \text{tgcgt}$  and  $[\text{CO}_2^-]$  conformers appear to contribute to the observed spectra with intensity changes indicating that there is more  $[\text{CO}_2^-]$  compared to  $[\text{N},\text{CO},\text{S}]$ , consistent with the changes in the relative energies calculated as a function of metal cation. The presence of  $[\text{COOH}]$  and  $[\text{COOH},\text{S}]$  conformers is again possible, although the peak corresponding to the carbonyl stretch provides no strong indications that these latter conformers are present.

#### Comparison of experimental and theoretical IR spectra: $\text{H}^+(\text{Met})$

Fig. 9 shows the IRMPD action spectrum of  $\text{H}^+(\text{Met})$  with theoretical predictions for three low-energy conformations. The  $\text{H}^+(\text{Met})$  complex is unique among all the systems investigated here as the proton is covalently bound to the amine group of the amino acid backbone. Only two spectra are shown for the four low-energy  $[\text{N},\text{CO},\text{S}]$  conformations described in Table 1 as the calculated IR spectra are identical for  $\text{tgttg}$  and  $\text{tgtgt}$  orientations and for  $\text{tgggg}$  and  $\text{tgggt}$  conformations. The calculated spectrum for the  $[\text{N},\text{OH},\text{S}] \text{tgttg}$  conformation is also shown for comparison. The experimental spectrum exhibits bands at 1775, 1560, 1455, 1330, 1230, 1155, 1050, 975, 865, 710, 620, and 580  $\text{cm}^{-1}$ . The observed peak at 1775  $\text{cm}^{-1}$  corresponds to the carbonyl stretch. The peaks at

1560 and 1455  $\text{cm}^{-1}$  correspond to the  $\text{NH}_3$  bending and  $\text{NH}_3$  umbrella motions, respectively. Observed bands at 1330 and 1230  $\text{cm}^{-1}$  correspond to wagging motions of the alpha carbon hydrogen atom and  $\text{CH}_2$  groups of the amino acid side chain. The  $\text{H}-\text{O}-\text{C}$  bending motion is represented by the peak observed at 1155  $\text{cm}^{-1}$ . The peak at 975 corresponds to elongation of the  $\text{C}-\text{C}$  and  $\text{C}-\text{N}$  bonds in the backbone, while the band at 865  $\text{cm}^{-1}$  corresponds to the  $\text{NH}_2$  rocking motion. The three peaks at 710, 620, and 580  $\text{cm}^{-1}$  are wagging motions of the acidic hydrogen atom.

The IRMPD action spectrum is well described by the  $[\text{N},\text{CO},\text{S}]$  calculated spectra. The  $\text{H}^+(\text{Met})$  carbonyl stretch in the observed spectrum (1775  $\text{cm}^{-1}$ ) is reproduced extremely well by the  $[\text{N},\text{CO},\text{S}]$  spectra (1768–1770  $\text{cm}^{-1}$ ), whereas the CO stretch is blue shifted nearly 45  $\text{cm}^{-1}$  (1820  $\text{cm}^{-1}$ ) for the  $[\text{N},\text{OH},\text{S}] \text{tgttg}$  conformer. Therefore, it is unlikely that the observed spectrum includes any contribution from the  $[\text{N},\text{OH},\text{S}]$  conformers, consistent with their calculated relative energies (Table 1), which would predict <0.5% population at 298 K. This peak is red shifted compared to the neutral ligand by much less than any of the metal cation complexes, consistent with a more delocalized charge in the  $\text{H}^+(\text{Met})$  complex. The bending and umbrella motions of the  $\text{NH}_3$  group in the calculated spectra for  $\text{H}^+(\text{Met})$  are blue shifted with respect to the observed peaks at 1455 and 1560  $\text{cm}^{-1}$ . This further illustrates that the single photon calculations cannot

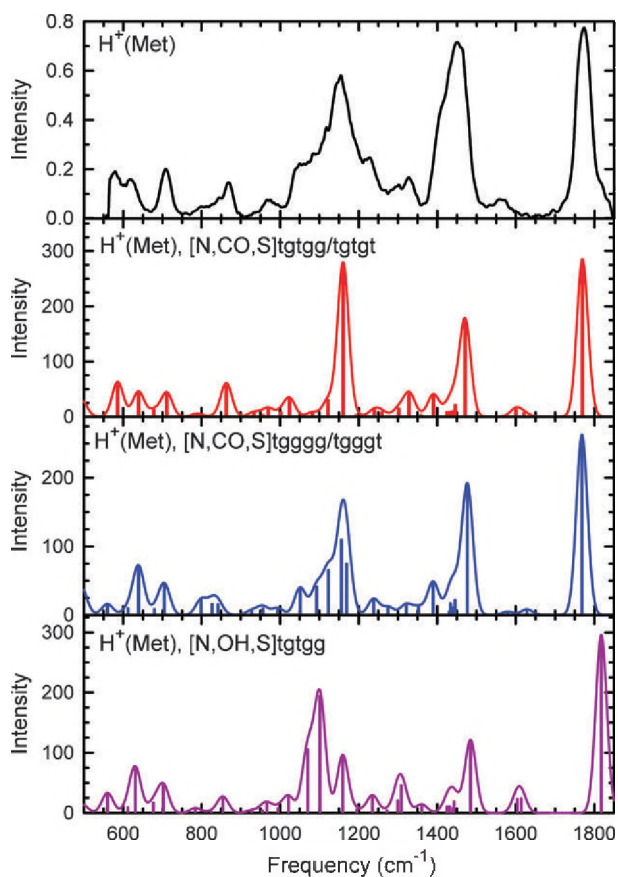


**Fig. 9** Comparison of the experimental IRMPD action spectrum for  $\text{H}^+(\text{Met})$  with IR spectra for two of the four lowest energy  $[\text{N},\text{CO},\text{S}]$  conformers and the lowest energy  $[\text{N},\text{OH},\text{S}]$  conformer predicted at the B3LYP/6-311+G(d,p) level of theory.

adequately describe the multiple photon spectra for umbrella or bending motions of the amine group. The broad peak spanning  $1375\text{--}1500\text{ cm}^{-1}$  in the observed spectrum is a conglomerate of the bands corresponding to the umbrella motions at  $1470\text{--}1475\text{ cm}^{-1}$  for the  $[\text{N},\text{CO},\text{S}]$  conformations, as well as the band at  $1390\text{ cm}^{-1}$ . The calculated spectra predict a band associated with the H–O–C bending mode at  $1160\text{ cm}^{-1}$ , which agrees with the  $1155\text{ cm}^{-1}$  peak in the observed spectrum. The large shoulder located at frequencies below the  $1155\text{ cm}^{-1}$  peak is reproduced by the shoulder of the  $\text{tgggg}/\text{tgggt}$  calculated spectrum, which indicates that these higher energy orientations are definitely present. The observed spectrum from  $580$  to  $1000\text{ cm}^{-1}$  is reproduced quite well by the  $[\text{N},\text{CO},\text{S}]$  calculated spectra. The band at  $865\text{ cm}^{-1}$  with a low frequency shoulder is consistent with the presence of both  $\text{tgtgg}/\text{tgtgt}$  and  $\text{tgggg}/\text{tgggt}$  orientations. The largest discrepancy in the low frequency region is the calculated band at  $640\text{ cm}^{-1}$  is blue shifted with respect to the observed peak at  $620\text{ cm}^{-1}$ . As noted above, the  $865\text{ cm}^{-1}$  band in the  $\text{H}^+(\text{Met})$  spectrum, which corresponds to the rocking motion of the  $\text{NH}_2$  group, does not appear in the  $\text{Li}^+(\text{Met})$  spectrum, Fig. 3. This is because the strong tridentate interaction of the lithium ion effectively quenches this rocking motion from occurring, whereas the bidentate interactions of the proton allow it.

### Overall comparison

We can now provide a more global comparison of the main features in all five spectra in Fig. 3. The predicted frequencies for the CO stretch of the  $[\text{N},\text{CO},\text{S}]\text{tgctg}$  conformer change from  $1705\text{ cm}^{-1}$  for  $\text{Li}^+(\text{Met})$ ,  $1721\text{ cm}^{-1}$  for  $\text{Na}^+(\text{Met})$ ,  $1728\text{ cm}^{-1}$  for  $\text{K}^+(\text{Met})$ ,  $1736\text{ cm}^{-1}$  for  $\text{Rb}^+(\text{Met})$ , and  $1739\text{ cm}^{-1}$  for  $\text{Cs}^+(\text{Met})$  ( $1732\text{ cm}^{-1}$  for the  $\text{tgggg}$  orientation), in agreement with the observed blue shift in the experimental spectra from  $1716\text{ cm}^{-1}$  for  $\text{Li}^+(\text{Met})$ ,  $1734\text{ cm}^{-1}$  for  $\text{Na}^+(\text{Met})$ ,  $1735\text{ cm}^{-1}$  for  $\text{K}^+(\text{Met})$ , and  $1742\text{ cm}^{-1}$  for both  $\text{Rb}^+(\text{Met})$  and  $\text{Cs}^+(\text{Met})$ . The CO stretch of the  $[\text{COOH}]$  conformers shows a similar shift with metal cation, changing from  $1733\text{--}1735\text{ cm}^{-1}$  for  $\text{K}^+$ ,  $1743\text{--}1745\text{ cm}^{-1}$  for  $\text{Rb}^+$ , and  $1746\text{--}1749\text{ cm}^{-1}$  for  $\text{Cs}^+$ ; however, because these bands are blue shifted compared to the  $[\text{N},\text{CO},\text{S}]$  conformer, appreciable contributions of the  $[\text{COOH}]$  conformers would be expected to lead to larger blue shifts in the experimental spectrum than observed. Likewise, the CO stretch for the  $[\text{COOH},\text{S}]$  conformers,  $1750\text{--}1756\text{ cm}^{-1}$  for  $\text{K}^+$ ,  $1747\text{--}1763\text{ cm}^{-1}$  for  $\text{Rb}^+$ , and  $1753\text{--}1764\text{ cm}^{-1}$  for  $\text{Cs}^+$ , is blue shifted even further, again suggesting that this species does not make major contributions to the experimental spectrum. The observed band at  $1158\text{ cm}^{-1}$  in the  $\text{Li}^+(\text{Met})$  spectrum red shifts to  $1145\text{ cm}^{-1}$  for  $\text{Cs}^+(\text{Met})$ . This shift is consistent with that predicted for the in-plane COH bending motion of  $[\text{N},\text{CO},\text{S}]\text{tgctg}$  conformers with predicted frequencies of  $1168\text{ cm}^{-1}$  for  $\text{Li}^+(\text{Met})$ ,  $1160\text{ cm}^{-1}$  for  $\text{Na}^+(\text{Met})$ ,  $1152\text{ cm}^{-1}$  for  $\text{K}^+(\text{Met})$ ,  $1148\text{ cm}^{-1}$  for  $\text{Rb}^+(\text{Met})$ , and  $1145\text{ cm}^{-1}$  for  $\text{Cs}^+(\text{Met})$ . Although the band at  $1595\text{ cm}^{-1}$  is not accurately predicted because of its anharmonicity, this band does not shift with metal cation identity, in agreement with the predictions for the  $[\text{N},\text{CO},\text{S}]\text{tgctg}$  conformers. No shifts are predicted for the broad band at  $1430\text{ cm}^{-1}$ , which becomes a high frequency shoulder in the spectra for  $\text{K}^+(\text{Met})\text{--}\text{Cs}^+(\text{Met})$ . Likewise the bands at about  $730\text{ cm}^{-1}$  observed in all the spectra are predicted to red shift somewhat, from  $738$  to  $724\text{ cm}^{-1}$  in going from  $\text{Li}^+(\text{Met})$  to  $\text{Cs}^+(\text{Met})$ . The good agreement in these trends provides further evidence that the  $[\text{N},\text{CO},\text{S}]\text{tgctg}$  conformer is present for all the IRMPD action spectra in Fig. 3.

The antisymmetric CO stretch of the  $[\text{CO}_2^-]$  conformers first appears in the IRMPD action spectrum for  $\text{Na}^+(\text{Met})$  at  $1650\text{ cm}^{-1}$  and blue shifts to  $1670\text{ cm}^{-1}$  for both  $\text{K}^+(\text{Met})$  and  $\text{Rb}^+(\text{Met})$ . This band is not as well defined for  $\text{Cs}^+(\text{Met})$ , but the photodissociation signal at similar frequencies can only be described by the presence of  $[\text{CO}_2^-]$  conformations. The predicted bands of all  $[\text{CO}_2^-]$  conformers agree well with the observed bands and are predicted to shift from  $1639$  to  $1661\text{ cm}^{-1}$  in going from  $\text{Na}^+(\text{Met})$  to  $\text{Rb}^+(\text{Met})$ . The umbrella motions of the  $\text{NH}_3$  group in the  $[\text{CO}_2^-]$  conformers are predicted at  $1417\text{--}1426\text{ cm}^{-1}$  for  $\text{K}^+(\text{Met})$ ,  $1408\text{--}1417\text{ cm}^{-1}$  for  $\text{Rb}^+(\text{Met})$ , and  $1402\text{--}1411\text{ cm}^{-1}$  for  $\text{Cs}^+(\text{Met})$ . This decrease in frequencies with heavier metal ion is consistent with the IRMPD action spectra for  $\text{K}^+(\text{Met})$ ,  $\text{Rb}^+(\text{Met})$ , and  $\text{Cs}^+(\text{Met})$  with peaks located at  $1405$ ,  $1395$ , and  $1390\text{ cm}^{-1}$ , respectively, Fig. 3, with a consistent shift to lower frequencies compared to experiment of  $\sim 15\text{ cm}^{-1}$ .

The theoretical results for  $\text{Rb}^+(\text{Met})$  and  $\text{Cs}^+(\text{Met})$  indicate that the  $[\text{COOH},\text{S}]$  and  $[\text{COOH}]$  conformers are low-energy

structures and could be present in the IRMPD action spectra. These conformers have intense bands predicted near  $1400\text{ cm}^{-1}$ , corresponding to the C–O–H bending motion, which are the most diagnostic bands in their calculated spectra. This motion is largely unaffected with increasing cation size for both conformers. For the [COOH.S] conformers, this motion is predicted at  $1378\text{--}1386\text{ cm}^{-1}$  for  $\text{K}^+$  (Met),  $1374\text{--}1389\text{ cm}^{-1}$  for  $\text{Rb}^+$  (Met), and  $1377\text{--}1386\text{ cm}^{-1}$  for  $\text{Cs}^+$  (Met). These predicted frequencies do lie closer to the observed peaks at  $1405$ ,  $1395$ , and  $1390\text{ cm}^{-1}$  for  $\text{K}^+$  (Met),  $\text{Rb}^+$  (Met), and  $\text{Cs}^+$  (Met), respectively, than the frequencies corresponding to the umbrella motion of the  $\text{NH}_3$  group in the  $[\text{CO}_2^-]$  conformers, but the frequencies increase as the metal gets heavier for the cgggg orientation and change very little for cgggt and cgccg orientations instead of the red shift experimentally observed. Likewise, the C–O–H bending modes of the [COOH] conformers are predicted to occur at  $1403\text{ cm}^{-1}$  for  $\text{K}^+$  (Met),  $1404\text{--}1410\text{ cm}^{-1}$  for  $\text{Rb}^+$  (Met), and  $1405\text{--}1407\text{ cm}^{-1}$  for  $\text{Cs}^+$  (Met). Because the observed bands at  $\sim 1400\text{ cm}^{-1}$  are broad in these three spectra, contributions from these two conformations cannot be eliminated.

## Conclusion

The IRMPD action spectra of cationized methionine in the region of  $550\text{--}1800\text{ cm}^{-1}$  have been obtained for complexes with  $\text{Li}^+$ ,  $\text{Na}^+$ ,  $\text{K}^+$ ,  $\text{Rb}^+$ ,  $\text{Cs}^+$ , and  $\text{H}^+$ . Comparison of these experimental spectra with IR spectra calculated at the B3LYP/6-311+G(d,p) and B3LYP/HW\*/6-311+G(d,p) levels of theory allow the conformations likely to be present in the experiment to be identified. For the  $\text{H}^+$  (Met) system, the IRMPD spectrum is characterized by four [N.CO.S] conformers that differ only in their side-chain orientation and therefore little in energy (within  $4\text{ kJ mol}^{-1}$ ). For the alkali-metal cationized systems, these comparisons suggest that the charge-solvated [N.CO.S] conformer is the only structure present in the IRMPD action spectrum for  $\text{Li}^+$  (Met) and  $\text{Na}^+$  (Met), consistent with it being the clear ground state conformation according to theory. This species remains a contributor for all metal cations studied. Contributions from the  $[\text{CO}_2^-]$  conformer, which becomes the ground state according to DFT calculations as the metal cation gets heavier, clearly manifest themselves for  $\text{K}^+$  (Met),  $\text{Rb}^+$  (Met), and  $\text{Cs}^+$  (Met). Theory suggests that [COOH.S], the ground state conformer for  $\text{Rb}^+$  (Met) and  $\text{Cs}^+$  (Met) according to MP2(full) calculations, and [COOH] conformers should also be present for  $\text{Rb}^+$  (Met) and  $\text{Cs}^+$  (Met). The experimental IRMPD action spectra cannot eliminate the presence of these conformers, but do not require their presence to be reproduced. The photodissociation spectra of  $\text{K}^+$  (Met),  $\text{Rb}^+$  (Met), and  $\text{Cs}^+$  (Met) have very similar spectral features and are considerably more complex than IRMPD spectra of  $\text{K}^+$ ,  $\text{Rb}^+$ , and  $\text{Cs}^+$  bound to other amino acids.<sup>3–8</sup>

## Acknowledgements

This work is part of the research program of FOM, which is financially supported by the Nederlandse Organisatie voor Wetenschappelijk Onderzoek (NWO). Additional financial

support was provided by the National Science Foundation, Grants PIRE-0730072 and CHE-0748790. The assistance of the FELIX staff is gratefully acknowledged.

## References

- 1 E. Wischmeyer, F. Doring and A. Karschin, *FEBS Lett.*, 2000, **466**, 115.
- 2 P. B. Armentrout, A. Gabriel and R. M. Moision, *Int. J. Mass Spectrom.*, 2009, **283**, 56.
- 3 P. B. Armentrout, M. T. Rodgers, J. Oomens and J. D. Steill, *J. Phys. Chem. A*, 2008, **112**, 2248.
- 4 M. T. Rodgers, P. B. Armentrout, J. Oomens and J. D. Steill, *J. Phys. Chem. A*, 2008, **112**, 2258.
- 5 M. W. Forbes, M. F. Bush, N. C. Polfer, J. Oomens, R. C. Dunbar, E. R. Williams and R. A. Jockusch, *J. Phys. Chem. A*, 2007, **111**, 11759.
- 6 A. L. Heaton, V. N. Bowman, J. Oomens, J. D. Steill and P. B. Armentrout, *J. Phys. Chem. A*, 2009, **113**, 5519.
- 7 M. F. Bush, J. Oomens, R. J. Saykally and E. R. Williams, *J. Phys. Chem. A*, 2008, **112**, 8578.
- 8 N. C. Polfer, J. Oomens and R. C. Dunbar, *Phys. Chem. Chem. Phys.*, 2006, **8**, 2744.
- 9 M. F. Bush, M. W. Forbes, R. A. Jockusch, J. Oomens, N. C. Polfer, R. J. Saykally and E. R. Williams, *J. Phys. Chem. A*, 2006, **111**, 7753.
- 10 J. J. Valle, J. R. Eyler, J. Oomens, D. T. Moore, A. F. G. van der Meer, G. von Helden, G. Meijer, C. L. Hendrickson, A. G. Marschall and G. T. Blakney, *Rev. Sci. Instrum.*, 2005, **76**, 023103.
- 11 N. C. Polfer and J. Oomens, *Phys. Chem. Chem. Phys.*, 2007, **9**, 3804.
- 12 N. C. Polfer, J. Oomens, D. T. Moore, G. von Helden, G. Meijer and R. C. Dunbar, *J. Am. Chem. Soc.*, 2006, **128**, 517.
- 13 D. Oepts, A. F. G. van der Meer and P. W. van Amersfoort, *Infrared Phys. Technol.*, 1995, **36**, 297.
- 14 R. M. Moision and P. B. Armentrout, *J. Phys. Chem. A*, 2002, **106**, 10350.
- 15 D. A. Pearlman, D. A. Case, J. W. Caldwell, W. R. Ross, T. E. Cheatham, S. DeBolt, D. Ferguson, G. Seibel and P. Kollman, *Comput. Phys. Commun.*, 1995, **91**, 1.
- 16 E. J. Bylaska, W. A. d. Jong, N. Govind, K. Kowalski, T. P. Straatsma, M. Valiev, D. Wang, E. Apra, T. L. Windus, J. Hammond, P. Nichols, S. Hirata, M. T. Hackler, Y. Zhao, P. D. Fan, R. J. Harrison, M. Dupuis, D. M. A. Smith, J. Nieplocha, V. Tipparaju, M. Krishnan, Q. Wu, T. V. Voorhis, A. A. Auer, M. Nooijen, E. Brown, G. Cisneros, G. I. Fann, H. Fruchtl, J. Garza, K. Hirao, R. Kendall, J. A. Nichols, K. Tsemekhman, K. Wolinski, J. Anchell, D. Bernholdt, P. Borowski, T. Clark, D. Clerc, H. Dachsel, M. Deegan, K. Dyall, D. Elwood, E. Glendening, M. Gutowski, A. Hess, J. Jaffe, B. Johnson, J. Ju, R. Kobayashi, R. Kutteh, Z. Lin, R. Littlefield, X. Long, B. Meng, T. Nakajima, S. Niu, L. Pollack, M. Rosing, G. Sandrone, M. Stave, H. Taylor, G. Thomas, J. van Lenthe and A. Wong, Z. Zhang, *NWChem, a Computational Chemistry Package for Parallel Computers*, Pacific Northwest National Laboratory, Richland, Washington, version 5.1 edn, 2007.
- 17 C. C. Roothaan, *Rev. Mod. Phys.*, 1951, **23**, 69.
- 18 J. S. Binkley, J. A. Pople and W. J. Hehre, *J. Am. Chem. Soc.*, 1980, **102**, 939.
- 19 M. J. Frisch, G. W. Trucks, H. B. Schlegel, G. E. Scuseria, M. A. Robb, J. R. Cheeseman, J. A. Montgomery, Jr., T. Vreven, K. N. Kudin, J. C. Burant, J. M. Millam, S. S. Iyengar, J. Tomasi, V. Barone, B. Mennucci, M. Cossi, G. Scalmani, N. Rega, G. A. Petersson, H. Nakatsuji, M. Hada, M. Ehara, K. Toyota, R. Fukuda, J. Hasegawa, M. Ishida, T. Nakajima, Y. Honda, O. Kitao, H. Nakai, M. Klene, X. Li, J. E. Knox, H. P. Hratchian, J. B. Cross, C. Adamo, J. Jaramillo, R. Gomperts, R. E. Stratmann, O. Yazyev, A. J. Austin, R. Cammi, C. Pomelli, J. W. Ochterski, P. Y. Ayala, K. Morokuma, G. A. Voth, P. Salvador, J. J. Dannenberg, V. G. Zakrzewski, S. Dapprich, A. D. Daniels, M. C. Strain,



- O. Farkas, D. K. Malick, A. D. Rabuck, K. Raghavachari, J. B. Foresman, J. V. Ortiz, Q. Cui, A. G. Baboul, S. Clifford, J. Cioslowski, B. B. Stefanov, G. Liu, A. Liashenko, P. Piskorz, I. Komaromi, R. L. Martin, D. J. Fox, T. Keith, M. A. Al-Laham, C. Y. Peng, A. Nanayakkara, M. Challacombe, P. M. W. Gill, B. Johnson, W. Chen, M. W. Wong, C. Gonzalez and J. A. Pople, *GAUSSIAN 03 (Revision D.01)*, Gaussian, Inc., Pittsburgh, PA, 2005.
- 20 A. D. Becke, *J. Chem. Phys.*, 1993, **98**, 5648.
- 21 R. Ditchfield, W. J. Hehre and J. A. Pople, *J. Chem. Phys.*, 1971, **54**, 724.
- 22 A. D. McLean and G. S. Chandler, *J. Chem. Phys.*, 1980, **72**, 5639.
- 23 R. Krishnan, J. S. Binkley, R. Seeger and J. A. Pople, *J. Chem. Phys.*, 1980, **72**, 650.
- 24 J. B. Foresman and A. E. Frisch, *Exploring Chemistry with Electronic Structure Methods*, Gaussian, Inc., Pittsburgh, PA, 2nd edn, 1996.
- 25 P. J. Hay and W. R. Wadt, *J. Chem. Phys.*, 1985, **82**, 299.
- 26 E. D. Glendening, D. Feller and M. A. Thompson, *J. Am. Chem. Soc.*, 1994, **116**, 10657.
- 27 F. Weigend and R. Ahlrichs, *Phys. Chem. Chem. Phys.*, 2005, **7**, 3297.
- 28 T. Leininger, A. Nicklass, W. Kuechle, H. Stoll, M. Dolg and A. Bergner, *Chem. Phys. Lett.*, 1996, **255**, 274.
- 29 M. F. Bush, J. Oomens, R. J. Saykally and E. R. Williams, *J. Am. Chem. Soc.*, 2008, **130**, 6463.
- 30 C. Y. Peng and H. B. Schlegel, *Isr. J. Chem.*, 1994, **33**, 449.
- 31 E. Stennett, D. R. Carl and P. B. Armentrout, work in progress.
- 32 N. N. Dookeran, T. Yalcin and A. G. Harrison, *J. Mass Spectrom.*, 1996, **31**, 500.
- 33 J. Oomens, D. T. Moore, G. Meijer and G. von Helden, *Phys. Chem. Chem. Phys.*, 2004, **6**, 710.
- 34 W. E. Sinclair and D. W. Pratt, *J. Chem. Phys.*, 1996, **105**, 7942.